

Stellar populations of cluster E and S0 galaxies

Inger Jørgensen^{★†}

McDonald Observatory, The University of Texas at Austin, RLM 15.308, Austin, TX 78712, USA

8 February 1997. Accepted for publication in MNRAS.

ABSTRACT

Spectral line index data for a sample of 290 E and S0 galaxies are used to investigate the stellar populations of these galaxies. 250 of the galaxies are members of 11 nearby clusters ($cz_{\text{CMB}} < 11500 \text{ km s}^{-1}$).

It is studied how the stellar populations of the galaxies are related to the velocity dispersions, the masses of the galaxies, and the cluster environment. This is done by establishing relations between these parameters and the line indices Mg_2 , $\langle \text{Fe} \rangle$ and $\text{H}\beta_{\text{G}}$. The difference between the slope of the Mg_2 - σ relation and the slope of the $\langle \text{Fe} \rangle$ - σ relation indicates that the abundance ratio $[\text{Mg}/\text{Fe}]$ is 0.3–0.4 dex higher for galaxies with velocity dispersions of 250 km s^{-1} compared to galaxies with velocity dispersions of 100 km s^{-1} . This is in agreement with previous estimates by Worthey et al.

The $\langle \text{Fe} \rangle$ index is stronger correlated with the projected cluster surface density, ρ_{cluster} , than with the galaxy mass or the velocity dispersion. We have earlier found the residuals for the Mg_2 - σ relation to depend on the cluster environment. Here we determine how both the Mg_2 index and the $\langle \text{Fe} \rangle$ index depend on the velocity dispersion and ρ_{cluster} . Alternative explanations that could create a spurious environment dependence are discussed. No obvious alternatives are found. The environment dependence of the Mg_2 - σ relation is supported by data from Faber et al. The dependence on the environment implies that $[\text{Mg}/\text{Fe}]$ decreases with increasing density, ρ_{cluster} . The decrease in $[\text{Mg}/\text{Fe}]$ is 0.1 dex over 2.5 dex in ρ_{cluster} .

We have also studied to what extent the mass-to-light (M/L) ratios of the galaxies are determined by the stellar populations. The M/L ratios are strongly correlated with the indices Mg_2 and $\text{H}\beta_{\text{G}}$, while the $\langle \text{Fe} \rangle$ index is only weakly correlated with the M/L ratio.

Based on current stellar population models we find that it is not yet possible to derive unique physical parameters (mean age, mean abundances, mean IMF, and fraction of dark matter) from the observables (line indices, velocity dispersion, mass, M/L ratio).

Key words: galaxies: elliptical and lenticular – galaxies: stellar content – galaxies: fundamental parameters – galaxies: scaling laws

1 INTRODUCTION

Optical studies of stellar populations in external galaxies beyond the Virgo cluster are limited to investigations based on the integrated light of the stars in smaller or larger parts of the galaxies. Radial gradients can be studied, but the individual stars cannot be resolved with present day instrumentation. The interpretation of the observations therefore relies on models of the stellar populations.

Since Baade (1944) introduced the idea of stellar populations in external galaxies broad band colors have been used for observational studies as well as modeling of stellar populations (e.g., Tinsley & Gunn 1976; Aaronson et al. 1978; Bruzual 1983; Buzzoni 1989, 1995; Bruzual & Charlot 1993; Peletier & Balcells 1996). More detailed studies are possible based on measurements of absorption features. In the Lick/IDS system indices are defined for lines in the optical region, 4100–6300 Å (Faber et al. 1985; Worthey et al. 1994). Line strengths for galaxies have been measured in this system by, e.g., Gorgas, Efstathiou & Aragón-Salamanca (1990), Worthey, Faber & Gonzáles (1992), Davidge (1992),

[★] E-mail: inger@roeskva.as.utexas.edu

[†] Hubble Fellow.

Davies, Sadler & Peletier (1993), Carollo, Danziger & Buson (1993), Fisher, Franx & Illingworth (1995, 1996) and Vazdekis et al. (1996ab).

Recent stellar population models have made predictions of the line indices in the Lick/IDS system, the broad band colors and the mass-to-light (M/L) ratio for single stellar populations (Buzzoni, Gariboldi & Mantegazza 1992; Worthey 1994; Buzzoni, Mantegazza & Gariboldi 1994; Vazdekis et al. 1996a; Bressan, Chiosi & Tantaló 1996). These models are static models in the sense that the aim is not to model the evolution of a stellar system, but to predict the observables for one stellar population with a given age, metallicity and initial mass function (IMF). Worthey and Bressan et al. use a Salpeter (1955) IMF, while Buzzoni et al. and Vazdekis et al. present models for several IMFs. Most of the available models use solar abundance ratios, specifically $[\text{Mg}/\text{Fe}]=0$. Current static models with $[\text{Mg}/\text{Fe}]=0$ fail to reproduce the observed flat relation between the magnesium index Mg_2 and the iron index $\langle \text{Fe} \rangle$ found for elliptical galaxies (Worthey et al. 1992; Buzzoni et al. 1994). Weiss et al. (1995) studied the effect of a non-solar $[\text{Mg}/\text{Fe}]$ and estimated that bright elliptical galaxies have $[\text{Mg}/\text{Fe}]$ in the interval $+0.3$ to $+0.7$.

Some authors have investigated the possibility of fitting evolutionary models to the stellar populations in elliptical galaxies. Even though beyond the scope of this paper, we note that the main problem is to create sufficiently enriched and old populations of stars that will fit the red colors and strong line indices characteristic for elliptical galaxies. Vazdekis et al. (1996ab) find that some process is needed to supply a strong enrichment early in the evolution of the galaxies. They argue that a time variable IMF may be feasible. Bressan et al. (1996) use an infall model to fit line index data from González (1993) and UV data from Burstein et al. (1988a).

Models of single stellar populations can be used to interpret the measured line indices and broad band colors in the sense that the “best fitting” model gives an estimate of the luminosity weighted mean age, mean metallicity and mean IMF of the current stellar populations. One of the problems with this technique is the degeneracy of the effects from variations in age and in metallicity. In general broad band colors cannot be used to disentangle age and metallicity effects (Aaronson et al. 1978; Worthey 1994). The possible presence of dust in E and S0 galaxies adds further confusion to the interpretation of broad band colors (e.g., Silva & Elston 1994). Many of the spectral indices defined in the Lick/IDS system suffer from the same degeneracy regarding age and metallicity. Worthey (1994) argues that $\text{H}\beta$ together with one of the magnesium indices can be used to break the degeneracy, since $\text{H}\beta$ is more sensitive to age than the magnesium indices. In later studies Jones & Worthey (1995) and Worthey, Trager & Faber (1995) use higher order Balmer lines together with several indices for heavier elements to estimate mean ages and metallicities for a sample of E galaxies. The current models are not in agreement with regard to the predicted near-infrared broad band colors. Peletier & Balcells (1996) find that near-infrared colors to some extent can be used to solve the age/metallicity degeneracy problem for E galaxies, while Worthey (1994) does not find near-infrared colors useful for breaking the degeneracy. The main cause of the differences in the near-infrared

colors is due to differences in the adopted models for the stellar evolution (Charlot, Worthey & Bressan 1996). None of the techniques for breaking the age/metallicity degeneracy takes variations in the abundance ratio $[\text{Mg}/\text{Fe}]$ into account.

Ideally one wants to use the observables (the line indices, the velocity dispersion, the M/L ratio, etc.) to derive physical parameters like the mean age, the mean abundances of various heavy elements, and the mean IMF for the stellar populations presently observed. In this context it should also be addressed what the fraction of dark matter is in the galaxies. If the fraction of dark matter is not the same in all E and S0 galaxies, this may give variations in the M/L ratio that are not reflected in the observed line indices.

In this paper spectroscopic data are analyzed for a large sample of cluster E and S0 galaxies. We concentrate on centrally measured indices aperture corrected to a standard size aperture. The aim is to establish empirical relations between the observables (the velocity dispersion; the line indices Mg_2 , $\text{H}\beta$ and $\langle \text{Fe} \rangle$; the M/L ratio; and the mass). The underlying physical questions are (a) whether the mix of stellar populations is determined by the velocity dispersion (or alternatively the mass), (b) which influence the cluster environment has, and (c) if the M/L ratio is determined by the stellar populations. The data are also compared to predictions from models of single stellar populations and the expected variations in the observables due to changes in the age, the abundances, the IMF, and the fraction of dark matter are discussed.

There are several studies of the Mg_2 - σ relation for large samples of E and S0 galaxies (Burstein et al. 1988b; Guzmán et al. 1992; Bender, Burstein & Faber 1993; Jørgensen, Franx & Kjaergaard 1996, hereafter Paper II). Relations that also involve $\text{H}\beta$ and $\langle \text{Fe} \rangle$ have previously only been studied for relatively small samples of galaxies (e.g., Gorgas et al. 1990; Worthey et al. 1992; Davies et al. 1993; González 1993; Worthey 1994; Fisher et al. 1995, 1996), though relations for a larger sample of E galaxies are shown by Burstein et al. (1984).

The present paper is organized as follows. Sect. 2 briefly describes the samples of galaxies. The determination of the line indices is covered by Sect. 3 and the Appendix. Sect. 4 has the empirical point of view. Linear relations between the available observables are established. It is also tested how the relations depend on the cluster environment. In Sect. 5 the data are compared with model predictions from stellar population models. The conclusions are summarized and discussed in Sect. 6.

Unless otherwise noted the relations established in this paper are determined by minimization of the sum of the absolute residuals perpendicular to the relations, and the zero points are derived as the median zero points. This fitting technique has the advantage that it is rather insensitive to a few outliers, and that it treats the coordinates in a symmetric way. The uncertainties of the coefficients are derived by a bootstrap procedure. See also Paper II for a discussion of this fitting technique.

Table 1. Number of E and S0 galaxies with available line indices

Cluster	H β _G	Mg ₂ ^a	<Fe>
Coma		80	
Abell 194	19	19	19
Abell 539	1	29	29
Abell 3381	16	16	16
Abell 3574	7	7	7
Abell S639	4	21	21
Abell S753	14	14	14
DC2345-28		10	
Doradus	8	8	8
Hydra I	12	42	42
Grm15	4	4	4
Cluster sample	85	250	160
Additional sample	40	40	39

Note – ^a Literature data for Mg₂ included, cf. Sect. 3.
 Mg₂ values derived from Mgb are also included.
 <Fe>=(Fe5270+Fe5335)/2.

2 SAMPLE SELECTION AND DATA

The observational data were originally obtained for our study of the Fundamental Plane for E and S0 galaxies in 11 nearby clusters (Paper II). The selection criteria for the galaxies are described in detail in Jørgensen, Franx & Kjaergaard (1995a) and Jørgensen & Franx (1994). The main selection criteria were classification (E or S0) and total magnitude. It should be noted that the samples are not complete to a well-defined absolute total magnitude. A representative lower limit on the luminosity of the galaxies in the sample is $M_{\text{rT}} = -20^{\text{m}}45$ in Gunn r ($H_0 = 50 \text{ km s}^{-1} \text{ Mpc}^{-1}$).

Photometry in Gunn r is taken from Jørgensen, Franx & Kjaergaard (1995a). The velocity dispersions and the Mg₂ indices are from Jørgensen, Franx & Kjaergaard (1995b, hereafter Paper I) and the literature, see Sect. 3. In Sect. 3 other line indices are derived from the same spectroscopic observations used in Paper I.

From the available data we define two samples. The “cluster sample” consists of the 250 E and S0 galaxies which are members of the 11 nearby clusters and for which we have at least the velocity dispersion and the Mg₂ index, see Table 1. Information about the cluster properties (radial velocity, richness, cluster velocity dispersion, etc.) is given in Paper II. 207 of the galaxies also have reliable photometry. (Though photometry is available for the galaxies Coma-D120 and Coma-D121 it is not used here, because the small angular distance between the two galaxies makes the photometric parameters highly uncertain.) The “additional sample” consists of the E and S0 galaxies observed for comparison purposes, some E and S0 galaxies in the Hickson (1982) compact groups, and observed E and S0 galaxies that turned out not to be members of the 11 nearby clusters. There are 40 galaxies in the additional sample. The cluster environments for these galaxies are in general less dense than for the galaxies in the cluster sample as most of the galaxies belong to small groups or the field.

Table 2. Number of measured indices and their median internal uncertainties

Index	N _{gal}	σ_{index}	$\sigma_{\log(\text{index})}$
Fe4531	27	0.46	0.072
C4668	58	0.70	0.043
H β	135	0.26	0.064
H β _G	131	0.17	0.038
Fe5015	213	0.47	0.039
Mg ₁	181	0.006	
Mg ₂	181	0.007	
Mgb	218	0.24	0.024
<Fe>	217	0.22	0.034
Fe5406	193	0.24	0.062
Fe5709	31	0.28	0.165
Fe5782	31	0.27	0.213
NaD	25	0.32	0.031

Note – <Fe>=(Fe5270+Fe5335)/2.

3 SPECTROSCOPIC DATA

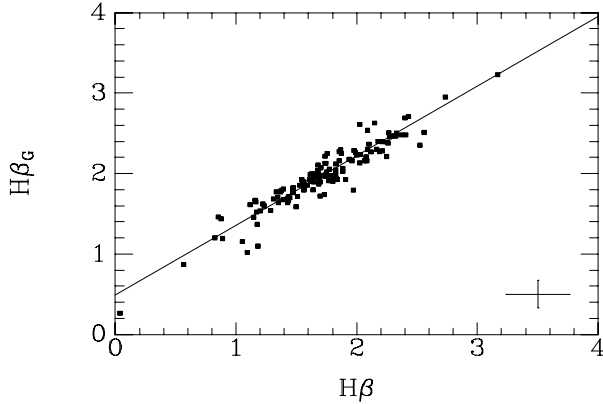
The spectra were obtained between 1990 and 1992 during three observing runs at the ESO 1.5m telescope equipped with the Boller & Chievens spectrograph (hereafter B&C) and one observing run at the ESO 3.6m telescope with the OPTOPUS instrument, a fiber-fed B&C spectrograph. Full information about the observing runs and the instrumentation is given in Paper I. The B&C spectra covered the wavelength interval 4700-5700Å or 4450-6160Å. The coverage for the OPTOPUS spectra was 5000-5620Å. The instrumental resolution was typically 1.25Å measured as sigma in a Gaussian fit to lines in a calibration spectrum. The typical signal-to-noise (S/N) ratio per Ångström is between 20 and 40. In total 220 galaxies were observed. Paper I describes the basic reduction of the spectra and the determination of radial velocities, velocity dispersions, and the Mg₂ index. The typical uncertainties derived from external comparisons are ± 0.036 for log σ and ± 0.013 for Mg₂, see Paper I. Here we determine the indices for additional absorption lines. The indices are derived from the flux calibrated spectra. We adopt the Lick/IDS definitions for the line indices (Worthey et al. 1994). The C4668 index is called Fe4668 by Worthey et al. We prefer to refer to it as C4668, because it is highly sensitive to the carbon abundance and not to the iron abundance (Tripicco & Bell 1995). Table 2 lists which indices have been measured and the number of galaxies for which it was possible to measure each index. The observations of S639-J31 and DC2345-28-D38 had too low S/N ratios to derive useful line indices. The median internal uncertainties based on the S/N ratio of the spectra are also given in the table.

The line indices were aperture corrected to a circular aperture with a metric diameter of $1.19h^{-1} \text{ kpc}$ ($H_0 = 100h \text{ km s}^{-1} \text{ Mpc}^{-1}$), equivalent to 3.4 arcsec at the distance of the Coma cluster. Further, the indices were corrected for the effect of the velocity dispersion, and they were calibrated to consistency with the Lick/IDS system. The corrections and calibration are described in the Appendix, which also contains tables of the final values.

For galaxies in Coma and DC2345-28 we have used literature data (log σ and Mg₂) from Davies et al. (1987), Dressler (1987), Lucey et al. (1991) and Guzmán et al. (1992). The data from the literature have been aperture corrected and transformed to a consistent system, see Paper I.

Table 3. Wavelength definition for $H\beta_G$

Index	Central passband	Continuum passbands
$H\beta_G$	4851.32 - 4871.32	4815.00 - 4845.00 4880.00 - 4930.00

**Figure 1.** The relation between the Lick/IDS $H\beta$ index and the $H\beta_G$ index. Typical error bars are given on the figure.

The typical measurement errors on the literature data are: $\log \sigma$, 0.025-0.036; and Mg_2 , ± 0.010 .

The magnesium indices Mgb , Mg_1 and Mg_2 are strongly correlated. The relations between the three indices do not have any significant intrinsic scatter, see Appendix. In the following only Mg_2 is used, since from an observational point of view no extra information is contained in Mgb and Mg_1 . For 37 galaxies without measured Mg_2 this index was derived from the measured Mgb , cf. Appendix.

3.1 Redefinition of the $H\beta$ index

The index for $H\beta$ as defined in the Lick/IDS system has very narrow continuum bands, 20Å and 15Å. This results in a relatively high uncertainty on the derived index. We have therefore experimented with a redefinition of the $H\beta$ index. We have adopted the same wavelength intervals for the $H\beta$ index as used by González (1993) for his emission line index, see Table 3. The index is in the following called $H\beta_G$. The central passband of $H\beta_G$ is narrower than the central passband for $H\beta$. This limits the contribution from the iron line which is within the passband of the Lick/IDS $H\beta$. Though the central passband for $H\beta_G$, like for the Lick/IDS definition, is too narrow to measure the real strength of the $H\beta$ line in A stars and hotter stars, the wider continuum bands give a better relative measure of the line strength. The main advantage of $H\beta_G$ is that the median uncertainty of $\log H\beta_G$ as derived from the S/N ratio of the spectra is 0.038, while the median uncertainty of $\log H\beta$ is 0.064. Naturally there is a tight correlation between $H\beta$ in the Lick/IDS system and the new $H\beta_G$. For the 129 galaxies with both indices measured and both positive we find

$$H\beta_G = 0.866 H\beta + 0.485 \pm 0.044 \quad (1)$$

with an rms scatter of 0.13, see Figure 1. Four galaxies have the blue continuum of $H\beta_G$ outside the wavelength range of the spectra, while it was possible to measure $H\beta$. For these galaxies Eq. 1 was used to transform $H\beta$ to $H\beta_G$. In the following analysis $H\beta_G$ is used in place of $H\beta$ and the model predictions of $H\beta$ are transformed to $H\beta_G$ using Eq. 1.

3.2 Emission lines

Many E and S0 galaxies are known to have emission lines from ionized gas especially in the central part of the galaxy (e.g., Davidge 1992; González 1993; Goudfrooij et al. 1994). Galaxies with significant emission from $[OIII]\lambda 5007$ and/or $H\beta$ are marked in Table A1. Based on the S/N of the spectra and on comparison with the data from González (1993) for the galaxies in common, we judge that emission in $[OIII]\lambda 5007$ with equivalent width larger than $\approx 0.5\text{Å}$ will be detected as significant emission. 16 galaxies in the cluster sample and 5 galaxies in the additional sample have significant emission.

The line indices $H\beta_G$, Fe5015, and to a smaller extent Mgb can be affected by emission. When $[OIII]$ emission is present also emission in $H\beta$ is present and will fill up the stellar $H\beta$ absorption line. The Fe5015 index has $[OIII]\lambda 5007$ in the central passband and $[OIII]\lambda 4959$ in the blue continuum passband. Since $[OIII]\lambda 5007$ is the stronger of the oxygen lines the index for Fe5015 will be weakened by the emission. The Mgb red continuum passband contains $[NI]\lambda 5198, 5200$. These lines are significantly weaker than $[OIII]\lambda 5007$. Goudfrooij & Emsellem (1996) find $[NI]\lambda 5198, 5200/[OIII]\lambda 5007 \approx 0.4$ for NGC2974. The effect of the emission is to make Mgb artificially stronger. We did not attempt to correct any of the line indices for emission. Instead galaxies with significant emission are omitted when relations that involve the $H\beta_G$ index are established.

4 THE EMPIRICAL POINT OF VIEW

An important question regarding galaxy evolution is which parameters determine the mix of stellar populations in E and S0 galaxies. In this section it is investigated to what extent the observed stellar populations of E and S0 galaxies are determined by the depth of the potential well of the galaxies, the mass of the galaxies and the cluster environment. The velocity dispersion is used as a measure of the depth of the potential well. Further, we study how well the M/L ratio is correlated with the stellar populations.

In order to characterize the stellar populations we need indices that will enable us to detect variations in age, metallicity and abundance ratios. We use Mg_2 , $\langle Fe \rangle$ and $H\beta_G$ as the primary indices. $H\beta_G$ is age sensitive, but also sensitive to the presence of blue horizontal branch stars (e.g., Bressan et al. 1996). Tripicco & Bell (1995) have studied how the Lick/IDS indices respond to changes in the abundances of various elements. They find that the Mg_2 index and the $\langle Fe \rangle$ index are mostly sensitive to the magnesium and the iron abundance, respectively. However, $\langle Fe \rangle$ is as sensitive to changes in the total metallicity as to changes in the iron abundance. The only index that reacts stronger to changes in the iron abundance than to changes in the total metallicity is Fe4383. This index cannot be measured from

Table 4. Model predictions from Vazdekis et al. (1996a)

Mg_2	\approx	$0.12 \log \text{age} + 0.19[M/H] + 0.14$
$\log <Fe>$	\approx	$0.12 \log \text{age} + 0.25[M/H] + 0.34$
$\log H\beta_G$	\approx	$-0.27 \log \text{age} - 0.135[M/H] + 0.51$
$\log M/L_r$	\approx	$0.63 \log \text{age} + 0.26[M/H] - 0.16$

Note – $[M/H] \equiv \log Z/Z_\odot$ is the total metallicity relative to solar.

our spectra because of their limited wavelength coverage. The Fe5406 index, which is also iron sensitive, is not used because the relative uncertainty on this index is larger than for $<Fe>$, cf. Table 2. We briefly discuss the C4668 index and the NaD index.

Models for single stellar populations like those by Vazdekis et al. (1996a) relate age and metallicity to expected values of the line indices and the M/L ratio. Table 4 lists approximate relations derived from these authors’ models with a bi-modal IMF with a Salpeter-like slope $\mu = 1.35$, and ages of 5Gyr or larger. The models have solar abundance ratios. However, to a first approximation we assume that the Mg_2 index and the $<Fe>$ index measure the magnesium abundance and the iron abundance, respectively. The relations in Table 4 are used in the following to quantify the changes in age and/or metallicity required to produce the ranges and offsets for the various indices.

4.1 The central velocity dispersion and the stellar populations

The velocity dispersion is known to correlate strongly with the Mg_2 index (e.g., Burstein et al. 1988b; Bender et al. 1993). Figure 2a shows this relation for the 250 E and S0 galaxies the cluster sample and for the 40 E and S0 galaxies in the additional sample. The relation derived in Paper II is overplotted. A fit to all the data in the cluster sample gives the same relation,

$$Mg_2 = 0.196 \log \sigma - 0.155 \pm 0.009 \quad (2)$$

with an rms scatter of 0.025. The coefficient given here is in agreement with determinations by Burstein et al. and Bender et al. The relation has an intrinsic scatter of 0.020 in Mg_2 .

The indices $H\beta_G$ and $<Fe>$ are also correlated with the velocity dispersion. Both the cluster sample and the additional sample were included in the analysis of these correlations. Because $<Fe>$ and $H\beta_G$ have relatively large measurement errors galaxies with uncertainty larger than 0.065 (15%) in $\log <Fe>$ and $\log H\beta_G$ are omitted from the analysis. For $H\beta_G$ also galaxies affected by emission are omitted.

The correlation between $<Fe>$ and σ is weak. A Spearman rank order test gives a probability of 0.18% that the parameters are not correlated. However, the correlation is driven by galaxies with either low or high velocity dispersion. If the sample is limited to galaxies with $\log \sigma$ in the interval from 2.0 to 2.4, there is no significant correlation between $<Fe>$ and $\log \sigma$. The galaxies with $\log \sigma$ in this interval have a mean $\log <Fe>$ of 0.455 with an rms scatter of 0.040. This agrees with the result from Fisher et al. (1996). These authors found for a relatively small sample of galaxies with velocity dispersions in the same interval that

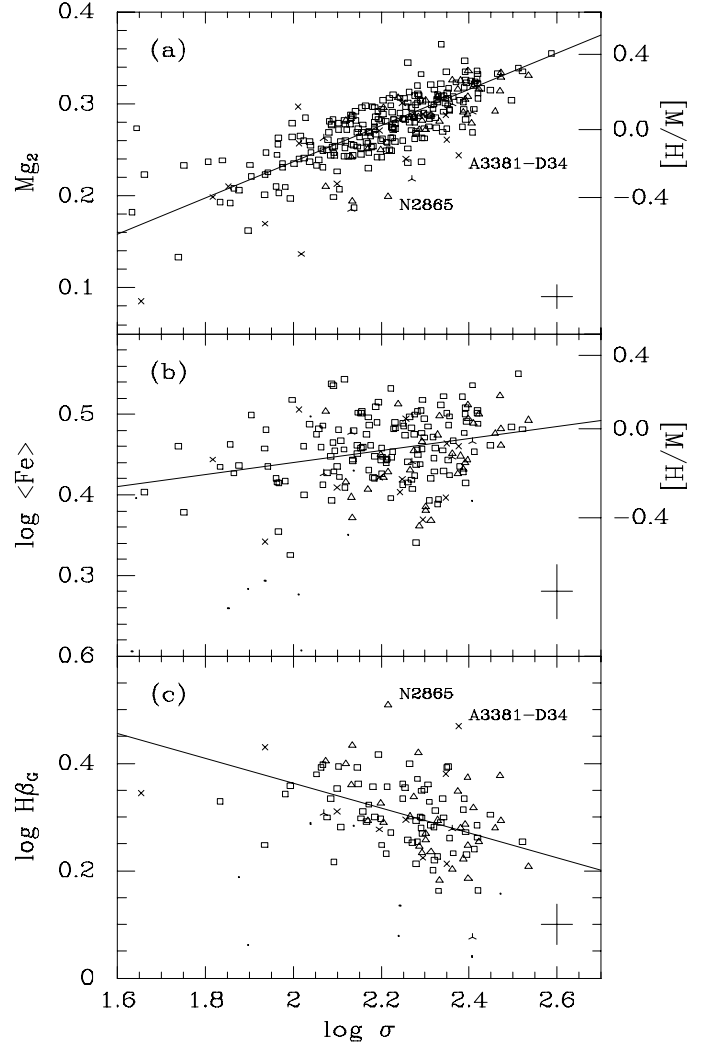


Figure 2. The line indices Mg_2 , $H\beta_G$ and $<Fe>$ versus the velocity dispersion. The $[M/H]$ axis on (a) and (b) shows the total metallicity relative to solar for single stellar population models from Vazdekis et al. (1996a). The models have a bi-modal IMF with slope $\mu = 1.35$ and an age of 12Gyr. Open symbols – galaxies without detected emission lines. Skeletal symbols – galaxies with significant emission lines. Four vertices – the cluster sample. Three vertices – the additional sample. On (b) and (c) galaxies for which the uncertainty is ≤ 0.065 on $\log <Fe>$ and $\log H\beta_G$, respectively, are shown as open or skeletal symbols. Typical error bars are given on the panels. Measurements with larger uncertainty are shown as points.

$<Fe>$ and σ were uncorrelated. For the full range of velocity dispersions we find

$$\log <Fe> = 0.075 \log \sigma + 0.291 \pm 0.025 \quad (3)$$

with an rms scatter of 0.041. 187 galaxies were included in the fit. The intrinsic scatter is 0.023. The relation is shown in Figure 2b. The rms scatter of $\log <Fe>$ for all 187 galaxies

is 0.043. Thus, the $\langle \text{Fe} \rangle$ - σ relation explains very little of the spread in the $\langle \text{Fe} \rangle$ indices.

The $[\text{M}/\text{H}]$ scales on Figure 2a and b show how $\langle \text{Fe} \rangle$ and Mg_2 depend on the total metallicity, $[\text{M}/\text{H}]$, for models with an age of 12 Gyr (Vazdekis et al. 1996a). $\langle \text{Fe} \rangle$ and Mg_2 react the same way to differences in age, cf. Table 4. Independent of the actual mean age of the galaxies the shallow slope of the $\langle \text{Fe} \rangle$ - σ relation compared to the Mg_2 - σ relation therefore shows that the abundance ratio $[\text{Mg}/\text{Fe}]$ must change with velocity dispersion. If the galaxies are coeval then $[\text{Mg}/\text{Fe}]$ may be 0.4 dex larger for galaxies with a velocity dispersion of 250 km s^{-1} than for galaxies with a velocity dispersion of 100 km s^{-1} , all caused by a change in the magnesium abundance. Since the $\langle \text{Fe} \rangle$ - σ relation may be flat for this interval of velocity dispersion, any increase in the mean age with velocity dispersion would have to be balanced with a decrease in the iron abundance. So even if the slope of the Mg_2 - σ relation was caused by age differences only, there would be an increase in $[\text{Mg}/\text{Fe}]$ of ≈ 0.3 dex between galaxies with $\sigma = 100 \text{ km s}^{-1}$ and galaxies with $\sigma = 250 \text{ km s}^{-1}$, caused by a decrease of the iron abundance. These results are similar to the results by Peletier (1989) and Worthey et al. (1992). Worthey et al. found the $[\text{Mg}/\text{Fe}]$ ratio to be larger than solar for galaxies with strong absorption lines.

The $\text{H}\beta_{\text{G}}$ index and the velocity dispersion show a strong correlation. A Spearman rank order test gives a probability of $< 0.01\%$ that σ and $\text{H}\beta_{\text{G}}$ are uncorrelated. We find

$$\log \text{H}\beta_{\text{G}} = -0.231 \log \sigma + 0.825 \pm 0.082 \quad (4)$$

with an rms scatter of 0.061. 101 galaxies were included in the fit. The intrinsic scatter is 0.047. The $\text{H}\beta$ - σ relation derived here is in agreement with the relations for E and S0 galaxies found by Fisher et al. (1995, 1996).

We note at this point, that the E and the S0 galaxies follow the same relations between the line indices and the velocity dispersion.

In order to study the influence of age variations on the scatter around the Mg_2 - σ relation and the $\langle \text{Fe} \rangle$ - σ relation we test if the galaxies that show emission lines are offset relative to the rest of the sample. The 21 galaxies with emission lines have a median offset in Mg_2 of -0.017 ± 0.009 and a median offset in $\log \langle \text{Fe} \rangle$ of -0.035 ± 0.022 relative to the relations given in Eq. 2 and Eq. 3, respectively. The emission lines are most likely caused by a young stellar population. The offsets are consistent with the mean age of these galaxies being ≈ 0.2 dex younger than the bulk of the galaxies.

The residuals for the Mg_2 - σ relation show a very weak correlation with $\log \text{H}\beta_{\text{G}}$ mostly driven by a few galaxies with very strong $\text{H}\beta_{\text{G}}$. The weak dependence on $\text{H}\beta_{\text{G}}$ may be seen in a direct determination of a relation between Mg_2 , $\log \sigma$ and $\text{H}\beta_{\text{G}}$. A least squares fit gives a coefficient for $\text{H}\beta_{\text{G}}$ which is significant on the 3σ level. If we instead minimize the sum of the absolute residuals in Mg_2 and determine the uncertainties by a boot strap procedure then the $\text{H}\beta_{\text{G}}$ is marginally significant. We find

$$\text{Mg}_2 = 0.209 \log \sigma - 0.056 \log \text{H}\beta_{\text{G}} - 0.173 \pm 0.014 \pm 0.042 \quad (5)$$

with an rms scatter of 0.019 in Mg_2 . The rms scatter of the the Mg_2 - σ relation is 0.020 for the same sample.

On Figure 2 the galaxies NGC2865 and A3381-D34 are labeled as examples of galaxies with weak Mg_2 and strong $\text{H}\beta_{\text{G}}$ for their velocity dispersion. The values of $\log \langle \text{Fe} \rangle$ for NGC2865 and A3381-D34 are fairly normal, 0.429 and 0.460 respectively. If the weak Mg_2 and strong $\text{H}\beta_{\text{G}}$ are due to young stellar populations in the galaxies, one expects that the $\langle \text{Fe} \rangle$ index is also weakened, cf. Table 4. It is not easy to understand why the $\langle \text{Fe} \rangle$ index has a fairly normal strength. This may indicate that some important clue is missing in our present interpretation of these indices.

The residuals for the Mg_2 - σ relation are neither correlated with $\log \langle \text{Fe} \rangle$ nor with the residuals for the $\langle \text{Fe} \rangle$ - σ relation. A fit of Mg_2 as function of both $\log \sigma$ and $\log \langle \text{Fe} \rangle$ gives a non-significant iron term. Thus, the residuals for the Mg_2 - σ relation seem unrelated to variations in the $\langle \text{Fe} \rangle$ index.

4.2 Effects of the cluster environment

In Paper II we found that the residuals for the Mg_2 - σ relation correlate with the cluster environment, specifically $\rho_{\text{cluster}} = \sigma_{\text{cluster}}^2 / R$. σ_{cluster} is the velocity dispersion of the cluster, and R is the cluster center distance of the galaxy. Thus, ρ_{cluster} is an estimate of the projected cluster surface density. A similar result was earlier found for the Coma cluster by Guzmán et al. (1992).

Figure 3 shows the residuals for the three relations, Mg_2 - σ , $\langle \text{Fe} \rangle$ - σ and $\text{H}\beta_{\text{G}}$ - σ , versus cluster center distance and versus ρ_{cluster} . The line indices Mg_2 , $\langle \text{Fe} \rangle$ and $\text{H}\beta_{\text{G}}$ are also plotted versus the cluster environment parameters. Both the cluster sample and the additional sample are shown. For 26 of the galaxies in the additional sample the environment parameters are derived based on cluster velocity dispersions from Faber et al. (1989) and Hickson et al. (1992), and redshifts from Maia et al. (1989). The field galaxies in the additional sample are separated from the other galaxies on the figure by a dashed line. These galaxies are not included in the analysis. None of the results change if all galaxies in the additional sample are excluded from the analysis.

There is a weak correlation between Mg_2 and ρ_{cluster} . We note that the velocity dispersions and ρ_{cluster} are not significantly correlated. The residuals for the Mg_2 - σ relation are strongly correlated with ρ_{cluster} , a Spearman rank order test gives a probability $< 0.01\%$ that there is no correlation (see also Paper II). This is in agreement with the result found by Guzmán et al. (1992) for the Coma cluster. For the 276 galaxies with all parameters we find

$$\text{Mg}_2 = 0.189 \log \sigma + 0.009 \log \rho_{\text{cluster}} - 0.196 \pm 0.012 \pm 0.002 \quad (6)$$

with an rms scatter of 0.024. The sum of the absolute residuals in Mg_2 was minimized. Eq. 6 agrees with our result from Paper II for a smaller sample of galaxies.

The data from Faber et al. (1989) for their 10 clusters with most observed galaxies and reliable cluster velocity dispersions show the same correlation between the residuals for the Mg_2 - σ relation and ρ_{cluster} , though the statistical significance is not as high as for our sample, see Figure 4. If we fit a relation similar to Eq. 6 to the data from Faber et al. the coefficient for ρ_{cluster} is significant on the 2σ level. Our analysis of the Faber et al. data included 143 galaxies in the

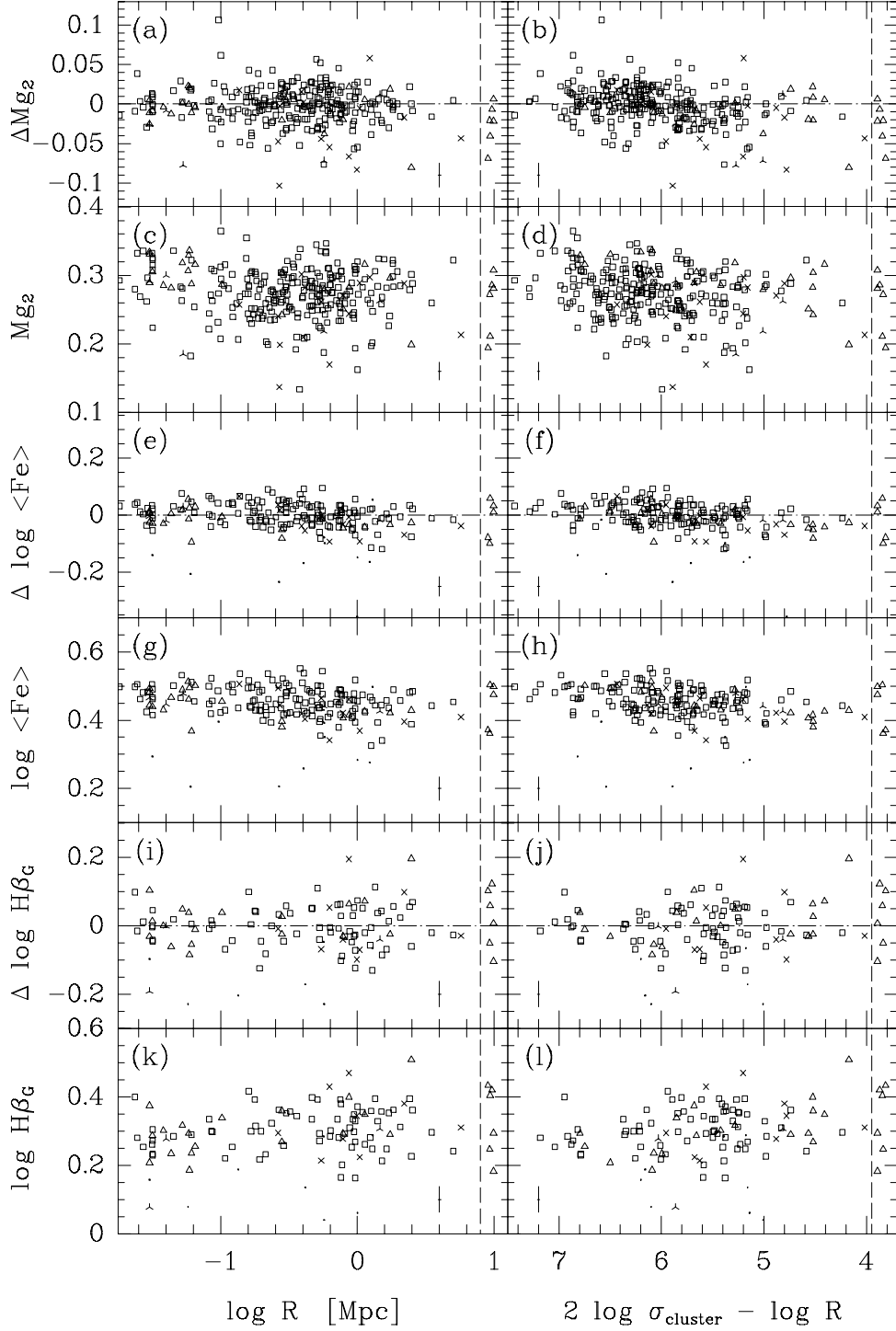


Figure 3. Residuals for the three relations, Mg_2 - σ , $\langle \text{Fe} \rangle$ - σ and $\text{H}\beta_G$ - σ , as well as the line indices versus cluster center distance, $\log R$, and versus $\log \rho_{\text{cluster}} = 2 \log \sigma_{\text{cluster}} - \log R$. ρ_{cluster} is an estimate of the local surface cluster density. The central parts of the clusters and the high density environments are to the left on the panels. Symbols as in Fig. 2. Field galaxies in the additional sample are plotted at random x -coordinates right of the dashed lines.

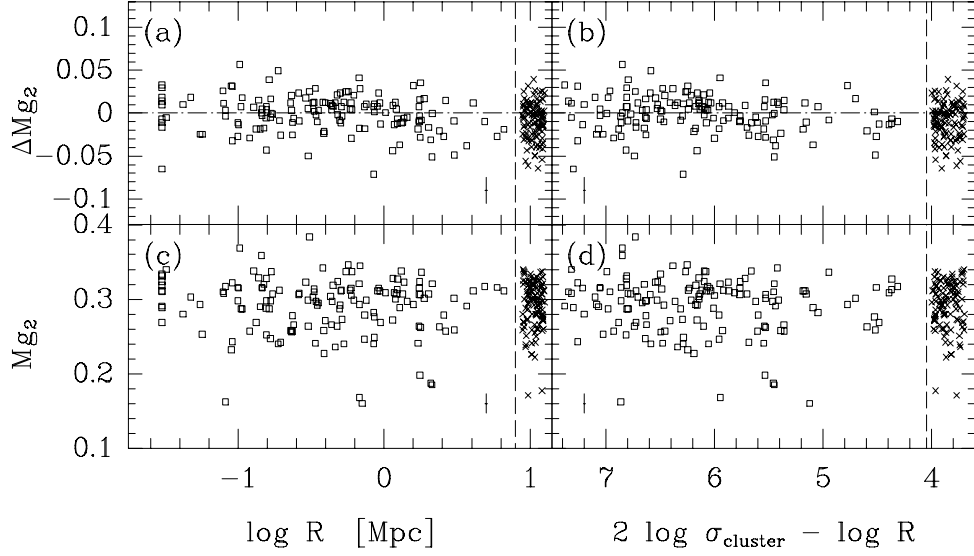


Figure 4. Data published by Faber et al. (1989). The figure shows the residuals for the Mg_2 - σ relation and the Mg_2 index versus cluster center distance, $\log R$, and versus $\log \rho_{\text{cluster}} = 2 \log \sigma_{\text{cluster}} - \log R$. Boxes – cluster galaxies; crosses – field galaxies, plotted at random x -coordinates right of the dashed lines.

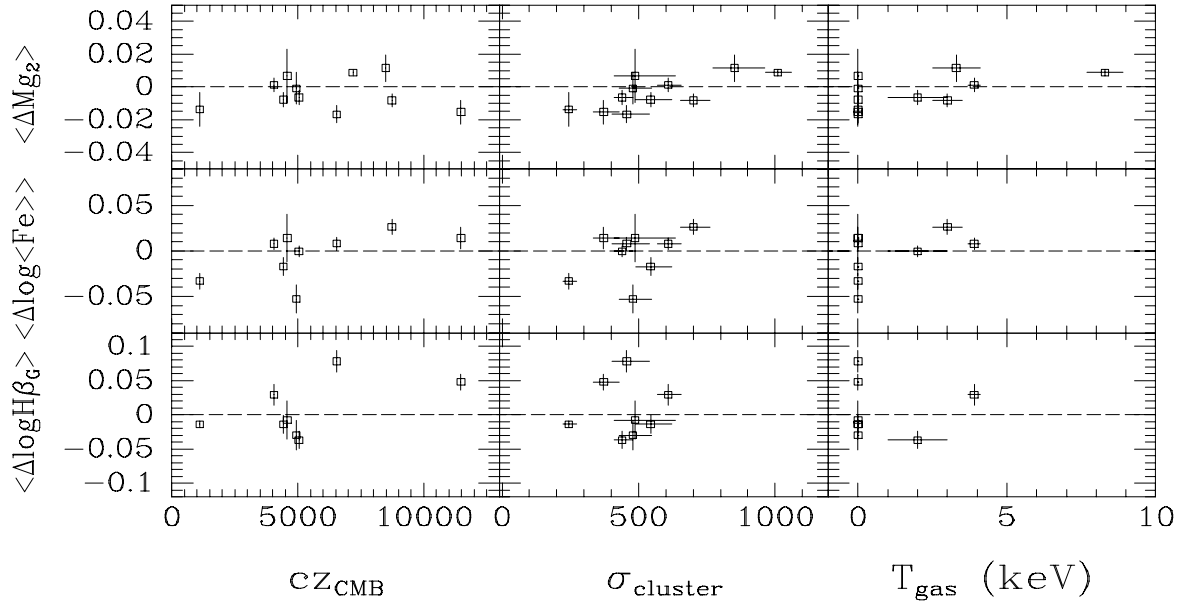


Figure 5. The median zero points for the Mg_2 - σ relation, the $\langle \text{Fe} \rangle$ - σ relation and the $H\beta_G$ - σ relation versus cluster parameters. σ_{cluster} is the velocity dispersion of the cluster. T_{gas} is the temperature of the X-ray gas in the cluster. The values of the cluster parameters are given in Paper II.

clusters A194, A2199, Antlia, DC2345-28, Coma, Eridanus, Fornax, Perseus, Pisces and Virgo.

Another way of testing the reality of the environment effect of the Mg_2 - σ relation is to compare field galaxies with cluster galaxies. The data from Faber et al. (1989) provide the largest homogeneous data base for such a test. We select as field galaxies all galaxies that according to Faber et al. are not members of any of the groups listed by these authors. Then we test if the residuals for the Mg_2 - σ relation for the 100 field galaxies selected this way and the 143 galaxies that are members of the clusters listed above are drawn from distributions with the same mean. A Mann-Whitney rank order test (van der Waerden 1969) gives a probability of only 0.3% that this is the case. The difference in the median zero points for the two samples of galaxies is 0.009 ± 0.003 . The field galaxies have slightly weaker Mg_2 than the cluster sample. The field galaxies are included on Figure 4, right of the dashed lines. See Burstein, Faber & Dressler (1990) and de Carvalho & Djorgovski (1992) for other discussions of the Mg_2 index for field and cluster galaxies.

The residuals for the $\langle \text{Fe} \rangle$ - σ relation correlate with both the cluster center distance and ρ_{cluster} . The same is the case for $\langle \text{Fe} \rangle$. A Spearman rank order test gives a probability $< 0.01\%$ that $\langle \text{Fe} \rangle$ and ρ_{cluster} are uncorrelated. In fact the $\langle \text{Fe} \rangle$ index correlates stronger with ρ_{cluster} than with any of the local parameters (velocity dispersion, M/L ratio and mass). The correlation is not weakened by exclusion of galaxies with $\log \sigma$ outside the interval 2.0–2.4. A relation between $\langle \text{Fe} \rangle$ and ρ_{cluster} also has slightly lower scatter than the $\langle \text{Fe} \rangle$ - σ relation. If we include both the velocity dispersion and ρ_{cluster} we find the following relation for the 174 galaxies with all parameters available and the uncertainty on $\log \langle \text{Fe} \rangle$ smaller than 0.065,

$$\log \langle \text{Fe} \rangle = 0.074 \log \sigma + 0.021 \log \rho_{\text{cluster}} + 0.170 \quad (7)$$

$$\pm 0.018 \quad \pm 0.004$$

The sum of the absolute residuals in $\log \langle \text{Fe} \rangle$ was minimized. The rms scatter of the relation is 0.038.

The residuals for the $\text{H}\beta_{\text{G}}$ - σ relation as well as $\text{H}\beta_{\text{G}}$ show no significant correlations with the environment (Figure 3i-l). We note, however, that galaxies with emission lines favor low density environments. A relation between $\text{H}\beta_{\text{G}}$, the velocity dispersion and ρ_{cluster} have a coefficient for $\log \rho_{\text{cluster}}$ of -0.011 ± 0.009 .

Figure 5 shows the median zero points for the relations between line indices and the velocity dispersion for each cluster versus cluster parameters. The slightly different values of $\langle \Delta \text{Mg}_2 \rangle$ compared to the similar figure in Paper II are due to the fact that the present work includes more galaxies. This does not change the result found in Paper II: A Kendall's τ correlation test shows that the correlation between $\langle \Delta \text{Mg}_2 \rangle$ and the cluster velocity dispersion is significant on the 96% level. Similar tests were performed for the median zero points for the $\langle \text{Fe} \rangle$ - σ relation and the $\text{H}\beta_{\text{G}}$ - σ relation, but showed no significant correlations with the cluster parameters.

4.2.1 Alternative explanations

Before we study the implications of the detected dependence of the environment, we discuss if it may be a spurious effect caused by either the corrections applied to the data or

inconsistencies between data from different sources. Eqs. 6 and 7 show that the changes in Mg_2 and $\log \langle \text{Fe} \rangle$ between $\log \rho_{\text{cluster}} = 7.0$ and 4.5 are -0.023 and -0.053 , respectively.

The velocity dispersion correction of Mg_2 is very small (< 0.003) and cannot cause the effects. The adopted aperture correction for Mg_2 is $0.04 \log(r_{\text{ap}}/r_{\text{norm}})$, cf. Appendix. The correction is largest for galaxies with radial velocities smaller than 2000 km s^{-1} . Most of these galaxies also happen to be in low density environments. The mean aperture correction for galaxies with $\text{cz}_{\text{CMB}} < 2000 \text{ km s}^{-1}$ and $\log \rho_{\text{cluster}} < 5.0$ is -0.024 . If the correct aperture correction is zero, the adopted correction could in principle create an offset in Mg_2 of this size. However, E and S0 galaxies are known to have radial gradients in Mg_2 , so a zero aperture correction is highly unlikely. Further, even if galaxies with $\text{cz}_{\text{CMB}} < 2000 \text{ km s}^{-1}$ are excluded from the analysis there is a strong correlation between ρ_{cluster} and the residuals for the Mg_2 - σ relation. The result by Guzmán et al. (1992) also supports that the adopted aperture correction did not create a spurious signal, since these authors' result is based on data for galaxies within one cluster and therefore does not depend critically on the adopted aperture correction.

The velocity dispersion correction of $\langle \text{Fe} \rangle$ is significant, 15% at $\sigma = 200 \text{ km s}^{-1}$ and 32% at $\sigma = 300 \text{ km s}^{-1}$. A high velocity dispersion makes the raw measurement value of the index smaller. The median correction for the galaxies in high density environments ($\log \rho_{\text{cluster}} > 6.5$) is 14.5%, while the median correction for galaxies in low density environments ($\log \rho_{\text{cluster}} < 5.0$) is 10%. The maximum difference in $\log \langle \text{Fe} \rangle$ between low and high density environments that this correction can cause is -0.02 . The aperture correction used for $\log \langle \text{Fe} \rangle$ is $0.05 \log(r_{\text{ap}}/r_{\text{norm}})$, cf. Appendix. The mean correction for galaxies with $\text{cz}_{\text{CMB}} < 2000 \text{ km s}^{-1}$ and $\log \rho_{\text{cluster}} < 5.0$ is -0.03 . Thus, in order to explain the detected change in $\log \langle \text{Fe} \rangle$ with environment as a spurious signal due to these corrections, both the velocity dispersion correction and the aperture correction for the index need to be zero. We do not find this very likely to be the case. E and S0 galaxies have radial gradients in $\langle \text{Fe} \rangle$, so some aperture correction is necessary. Further, our correction for the velocity dispersion agrees with similar corrections used by Davies et al. (1993). Finally, the galaxies with $\text{cz}_{\text{CMB}} > 2000 \text{ km s}^{-1}$ show just as strong a correlation between $\langle \text{Fe} \rangle$ and ρ_{cluster} as the full sample.

The adopted aperture corrections for the line indices are based on average radial gradients of the indices, cf. Appendix. E and S0 galaxies show a significant spread in the radial gradients of Mg_2 and $\log \langle \text{Fe} \rangle$ (e.g., Davies et al. 1993; Carollo et al. 1993; Fisher et al. 1995, 1996). If the radial gradients depend on the cluster environment then this may result in a spurious environment dependence for centrally measured indices aperture corrected with this technique. Radial gradients of the line indices are not available for the present sample, so a direct test cannot be performed. However, Carollo et al. (1993) found for galaxies with masses smaller than $10^{11} M_{\odot}$ that the radial gradient of Mg_2 was correlated with the galaxy mass, the velocity dispersion, and possibly with the luminosity and the ellipticity. If any of these parameters are correlated with the cluster center distance or with ρ_{cluster} this may also be the case for the radial gradients of Mg_2 (and possibly $\log \langle \text{Fe} \rangle$). For the samples of galaxies used in the present analysis Spearman

rank order tests show no significant correlations between the cluster environment parameters (cluster center distance and ρ_{cluster}) and the masses, the absolute luminosities, the effective radii in kpc, the velocity dispersions or the ellipticities of the galaxies. Further, there are no significant differences in the median values of these parameters for the galaxies in high density environments ($\log \rho_{\text{cluster}} > 6.5$) and in low density environments ($\log \rho_{\text{cluster}} < 5.5$). It should also be noted that the range in the Mg_2 gradients for galaxies with masses larger than $10^{11} M_{\odot}$ is as large as the range for the low mass galaxies (cf. Carollo et al. 1993). Thus, it does not seem likely that environment dependences for some of the structural parameters cause spurious environment dependences for the Mg_2 and $\langle \text{Fe} \rangle$ indices.

The Mg_2 indices for galaxies in Coma and DC2345-28 are from the literature. Our data for the clusters Hydra I, A539, A3381 and S639 were mostly taken with the OPTOPUS instrument, while the rest of our data are from B&C spectra. Despite the best efforts there may be inconsistencies between the literature data, the OPTOPUS data and the B&C data. It was therefore tested if the environment dependences can be detected from subsamples restricted to one or two sources of data. For the Mg_2 index we test the literature data alone, our data alone, and our data divided in OPTOPUS and B&C data as outlined above. The residuals for the Mg_2 - σ relation show no dependence on the environment based on the literature data alone. This is expected since this subsample consists of the two richest and most dense clusters, and the range in cluster center distances is rather limited. For our data alone a Spearman rank order test gives a probability of $P=0.6\%$ that the residuals are uncorrelated with ρ_{cluster} . For the subsamples of OPTOPUS and B&C data the probabilities are 1.5% and 24%, respectively. For all subsamples of our data the coefficient for $\log \rho_{\text{cluster}}$ is consistent with Eq. 6. The comparisons of the Mg_2 indices from different sources, see Paper I, did not indicate any large systematic problems. The results from the subsamples also support that the environment effect is real. We will caution though, that we cannot totally rule out that part of the detected environment effect for the Mg_2 index is spurious and caused by inconsistencies between the different data sources.

All the determinations of the $\langle \text{Fe} \rangle$ index come from our observations. We divide the sample in two subsamples consisting of the OPTOPUS data and the B&C data, respectively. The probability that $\langle \text{Fe} \rangle$ and ρ_{cluster} are uncorrelated is 0.8% for the OPTOPUS data and 0.03% for the B&C data. For both subsamples the coefficient for $\log \rho_{\text{cluster}}$ is consistent with Eq. 7. Because the environment effect for the $\langle \text{Fe} \rangle$ index is clearly detectable in both subsamples, we see no indications that this effect is caused by inconsistencies in the data.

4.2.2 Implications of the environment effects

If the changes in Mg_2 and $\langle \text{Fe} \rangle$ with ρ_{cluster} are interpreted as a change in the abundances only, this implies that $[\text{Mg}/\text{H}]$ increases with 0.12 dex and $[\text{Fe}/\text{H}]$ increases with 0.22 dex, as the density $\log \rho_{\text{cluster}}$ increases from 4.5 to 7 (cf. Table 4). This means the abundance ratio $[\text{Mg}/\text{Fe}]$ must decrease with ≈ 0.1 dex between $\log \rho_{\text{cluster}} = 4.5$ and 7. Because Mg_2 and $\log \langle \text{Fe} \rangle$ are equally sensitive to age variations it

is not possible with the current models to avoid a decrease in $[\text{Mg}/\text{Fe}]$ for high density environments relative to low density environments. Even if the full change in Mg_2 is caused by age variations $[\text{Fe}/\text{H}]$ must increase with ≈ 0.1 dex, thus giving the same decrease in $[\text{Mg}/\text{Fe}]$ as found above. We note, however, that it is not likely that the change in Mg_2 is caused by age variations only, since this would lead to a too large change of the M/L ratio of the galaxies as function of the environment (see Paper II). Further, the required increase in age of 0.18 dex would give a change in $\log H\beta_G$ of ≈ -0.05 . This is consistent with the data, though only marginally.

The environment dependence we find for the Mg_2 index and the $\langle \text{Fe} \rangle$ index adds to the growing evidence that the stellar populations in E and S0 galaxies are influenced by the surrounding environment (e.g., Guzmán et al. 1992; de Carvalho & Djorgovski 1992; Rose et al. 1994). The real picture of the environmental effects is most likely much more complex than a simple gradient with cluster center distance and/or ρ_{cluster} . The analysis presented here does not take sub-clustering into account; an effect known to be present and related to recent star formation in galaxies in the Coma cluster (Caldwell et al. 1993). There may also be differences between clusters of similar richness.

It should be emphasized that the galaxy sample used for this analysis is by no means complete and the results should be tested for a complete sample of galaxies. It would be very valuable to get $\langle \text{Fe} \rangle$ and $H\beta_G$ for galaxies in Coma and DC2345-28, the two richest clusters in our sample.

4.3 Relations between line indices

Since all three indices Mg_2 , $\langle \text{Fe} \rangle$ and $H\beta_G$ are correlated with the velocity dispersion it is also expected that they are correlated with each other. A Spearman rank order test gives a 0.17% probability that Mg_2 and $\langle \text{Fe} \rangle$ are uncorrelated, and a probability $< 0.01\%$ that Mg_2 and $H\beta$ are uncorrelated. Because of the shallow slopes and the large scatter of these relations they are derived by minimization of the sum of the absolute residuals in $\log \langle \text{Fe} \rangle$ and $\log H\beta_G$, respectively. The same galaxies were included as for the determination of Eq. 3 and Eq. 4, respectively. The two relations are shown in Figure 6. The derived relations agree within the uncertainties with those for E galaxies given by Burstein et al. (1984), see Figure 6.

In Sect. 4.1 we showed that the correlation between $\langle \text{Fe} \rangle$ and the velocity dispersion is driven by galaxies that have either low or high velocity dispersion. This is also the case for the correlation between $\langle \text{Fe} \rangle$ and Mg_2 . The galaxies with $\log \sigma$ in the interval 2.0–2.4 show no significant correlation between $\langle \text{Fe} \rangle$ and Mg_2 . This emphasizes that the magnesium abundance and the iron abundance seem to be only loosely connected, in agreement with their different dependence on the velocity dispersion (Sect. 4.1).

The residuals for the $\langle \text{Fe} \rangle$ - Mg_2 relation are dependent on the cluster environment in a similar way as the residuals for the $\langle \text{Fe} \rangle$ - σ relation. A fit that involves both line indices and ρ_{cluster} gives

$$\log \langle \text{Fe} \rangle = \begin{matrix} 0.26 \text{ Mg}_2 + 0.022 \log \rho_{\text{cluster}} + 0.261 \\ \pm 0.13 \quad \quad \pm 0.006 \end{matrix} \quad (8)$$

for the 174 galaxies with reliable cluster parameters. The

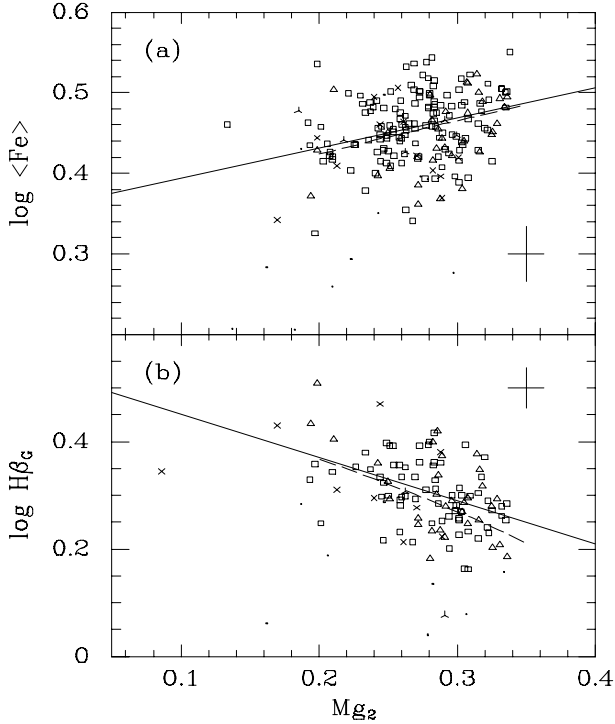


Figure 6. The relations between Mg_2 , $H\beta_G$ and $\langle Fe \rangle$. Symbols as in Fig. 2. Typical error bars are given on the panels. Solid lines – relations derived here. $\log \langle Fe \rangle = (0.37 \pm 0.11)Mg_2 + 0.36$, 187 galaxies, $rms=0.041$. The intrinsic scatter is 0.022. $\log H\beta_G = (-0.81 \pm 0.20)Mg_2 + 0.53$, 101 galaxies, $rms=0.059$. The intrinsic scatter is 0.044. Dashed lines – relations from Burstein et al. (1984).

relation has an rms of 0.038 in $\log \langle Fe \rangle$. This relation confirms the environment dependence of $[Mg/Fe]$ discussed in Sect. 4.2.2. Eq. 8 shows that for a given value of Mg_2 the $\langle Fe \rangle$ index increases with the cluster density, and therefore $[Mg/Fe]$ must decrease.

We do not find any environment dependence of the residuals for the $H\beta_G$ - Mg_2 relation. Because of the slope of the relation variations in the metallicity will not contribute to the scatter. Thus, if the environment dependence of Mg_2 discussed in Sect. 4.2 is caused by changes in the metallicity then no environment dependence of the residuals for the $H\beta_G$ - Mg_2 relation is expected.

$\langle Fe \rangle$ and $H\beta_G$ are not correlated; a Spearman rank order test gives a 68% probability that the parameters are uncorrelated. The residuals for the $\langle Fe \rangle$ - Mg_2 relation are not significantly correlated with $H\beta_G$, and the residuals for the $H\beta_G$ - Mg_2 relation are not significantly correlated with $\langle Fe \rangle$. Based on this a combination of Mg_2 and $\langle Fe \rangle$ is not expected to give tighter correlation with $H\beta_G$ than Mg_2 alone. For the sample of 100 galaxies with all indices available and no significant emission we find

$$\log H\beta_G = -1.02Mg_2 + 0.45 \log \langle Fe \rangle + 0.39 \quad (9)$$

$\pm 0.21 \quad \pm 0.23$

The sum of the absolute residuals in $\log H\beta_G$ were minimized. The coefficient for $\langle Fe \rangle$ is significant on the 2σ

level, The rms scatter is 0.056, thus the relation does not improve the scatter significantly.

Fisher et al. (1995) fit the quotient $Mgb/Fe5270$ as function of $H\beta$ for a smaller sample of E galaxies. The signs for the dependence on the magnesium and the iron indices given in Eq. 9 are in agreement with the result from Fisher et al. Eq. 9, however, shows that the $H\beta$ depends stronger on the Mg_2 index than on the $\langle Fe \rangle$ index. Fisher et al. were specifically testing if $H\beta$ was determined by the ratio $Mgb/Fe5270$ and therefore explicitly assumed that the dependences of the magnesium index and of the iron index had the same strength.

4.4 The M/L ratio, the mass and the stellar populations

Next we investigate the correlations between the line indices and the M/L ratio and the mass of the galaxies. Only the cluster sample is used for this analysis. In Paper II we found that for a given mass (or velocity dispersion) the M/L ratio is determined to 0.1 dex (see also Renzini & Ciotti 1993). It must imply that the stellar population is a very strong function of the mass (or velocity dispersion).

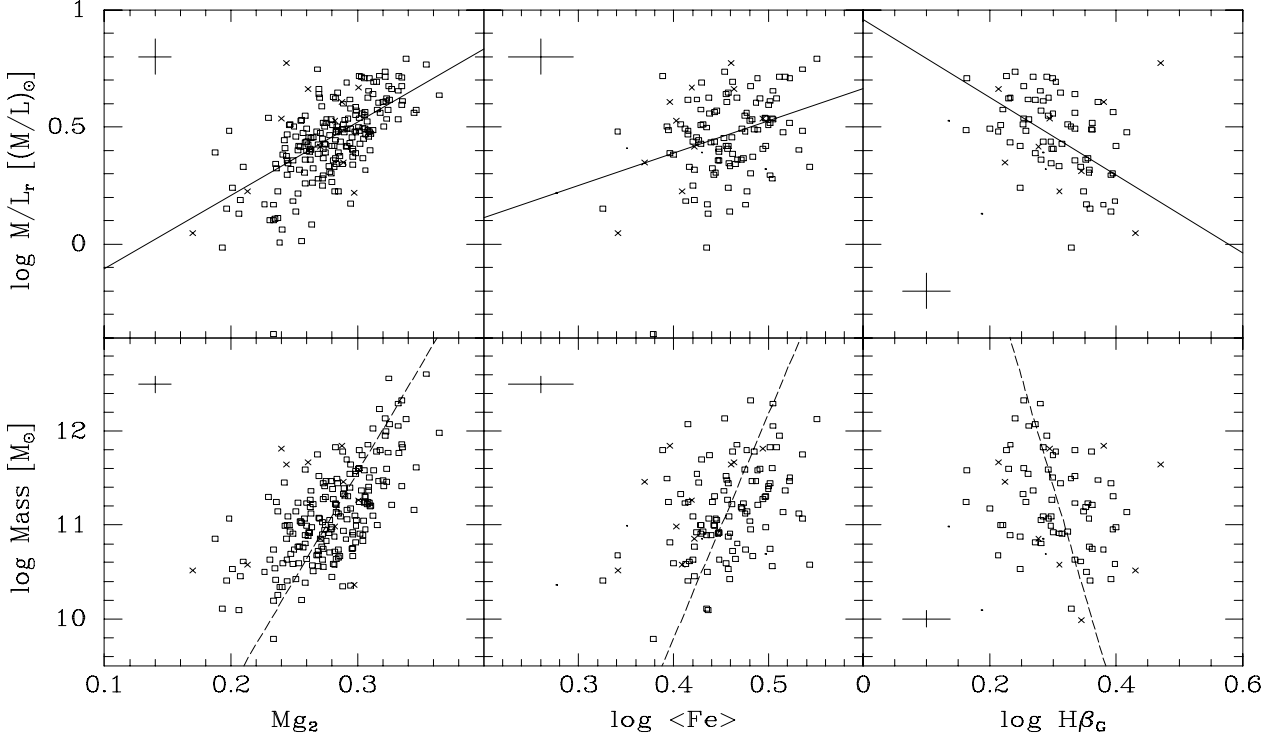
The M/L ratio in Gunn r in solar units is determined as $\log M/L_r = 2 \log \sigma - \log \langle I \rangle_e - \log r_e - 0.73$ ($H_0 = 50 \text{ km s}^{-1} \text{ Mpc}^{-1}$), with $\text{Mass} = 5\sigma^2 r_e / G$ (cf. Paper II). r_e is the effective radius in kpc, and $\langle I \rangle_e$ is the mean surface brightness within r_e in L_\odot/pc^2 . Because the determinations of the M/L ratios and the masses use the distance estimates based on the Fundamental Plane (FP) ($\log r_e = 1.24 \log \sigma - 0.82 \log \langle I \rangle_e + \gamma_{cl}$, see Paper II), it is implicitly assumed that the FP does not depend on the environment. This means it will not be possible to detect any environment dependence of relations that involve the M/L ratios or the masses, even though such a dependence is expected for the M/L ratios when the Mg_2 - σ relation and the $\langle Fe \rangle$ - σ relation depend on the environment.

The line indices Mg_2 , $\langle Fe \rangle$ and $H\beta_G$ are all correlated with the M/L ratios and with the masses of the galaxies. The probabilities that the parameters are uncorrelated as derived from Spearman rank order tests are given in Table 5, together with the derived relations. The relations are derived by minimization of the sum of absolute residuals in either the M/L ratio or the line index, as listed in the table. Figure 7 shows the data with the relations overplotted. Galaxies with measurement errors larger than 0.065 on $\log \langle Fe \rangle$ and $\log H\beta_G$ were omitted from the determinations of the relations for these line indices. For relations that involve $H\beta_G$ galaxies with significant emission were omitted.

The correlations of the $\langle Fe \rangle$ index with the M/L ratio and the mass are, like the correlations of $\langle Fe \rangle$ with the velocity dispersion and with the Mg_2 index, driven by galaxies with either low or high velocity dispersion. For the galaxies with $\log \sigma$ in the interval 2.0–2.4 the $\langle Fe \rangle$ index is not significantly correlated with neither the M/L ratio nor the mass. Thus, for these galaxies the mass does not determine the $\langle Fe \rangle$ index, and the $\langle Fe \rangle$ index does not influence the M/L ratio. On the other hand, the correlations between the Mg_2 index and the M/L ratio and the mass are very tight. This shows in agreement with the results from the previous sections that the $\langle Fe \rangle$ index is not governed by the same quantities that affect the Mg_2 index. The Mg_2

Table 5. Relations for the M/L ratio and the mass

Relation	N_{gal}	rms	rms _{int}	min.coord.	P
$\log M/L_r = (3.13 \pm 0.41)\text{Mg}_2 - 0.42$	207	0.14	0.11	$\log M/L_r$	< 0.01%
$\text{Mg}_2 = (0.044 \pm 0.004) \log \text{Mass} - 0.205$	207	0.028	0.024	Mg_2	< 0.01%
$\log M/L_r = (1.37 \pm 0.50) \log \langle \text{Fe} \rangle - 0.16$	114	0.17	0.14	$\log M/L_r$	0.2%
$\log \langle \text{Fe} \rangle = (0.042 \pm 0.011) \log \text{Mass} - 0.008$	114	0.041	0.023	$\log \langle \text{Fe} \rangle$	0.01%
$\log M/L_r = (-1.66 \pm 0.51) \log \text{H}\beta_{\text{G}} + 0.96$	67	0.15	0.11	$\log M/L_r$	0.01%
$\log \text{H}\beta_{\text{G}} = (-0.043 \pm 0.014) \log \text{Mass} + 0.791$	67	0.057	0.042	$\log \text{H}\beta_{\text{G}}$	1.3%

**Figure 7.** The line indices versus the M/L ratio and the mass of the galaxies in the cluster sample. Symbols as in Fig. 2. Typical error bars are given on the panels. Solid lines – relations with residuals minimized in $\log M/L_r$. Dashed lines – relations with residuals minimized the line indices. The relations are listed in Table 5.

index is nearly fully determined by the velocity dispersion (or the mass) of the galaxies, $\langle \text{Fe} \rangle$ is not.

For this sample of galaxies the velocity dispersion and the mass of a galaxy are equally good determinators of the $\text{H}\beta_{\text{G}}$ index, since the scatter of the two relations is approximately the same. The M/L ratio is strongly affected by $\text{H}\beta_{\text{G}}$; as expected if a strong $\text{H}\beta_{\text{G}}$ is caused by a young stellar population.

All the relations for the M/L ratio have significant intrinsic scatter, cf. Table 5. The scatter in the M/L ratio at a given line strength is 0.14–0.17 dex, the corresponding intrinsic scatter is 0.11–0.14 dex. For the sample of 67 galaxies without significant emission and for which good determinations of all the parameters are available we have tested if a combination of the three line indices will give a tighter correlation with the M/L ratio than the relations given in Table 5. A combination of Mg_2 and $\langle \text{Fe} \rangle$ gives a non-significant iron term and the scatter in the M/L ratio is the same as for the relation between the M/L ratio and Mg_2 . A combination

of $\langle \text{Fe} \rangle$ and $\text{H}\beta_{\text{G}}$ does give significant coefficients for both terms, but the scatter is not improved compared to relations that involve only one of the indices. The best relation is for a combination of Mg_2 and $\text{H}\beta_{\text{G}}$. We minimize the sum of the absolute residuals in the M/L ratio and find

$$\log M/L_r = \begin{matrix} 3.31\text{Mg}_2 - 0.62\log \text{H}\beta_{\text{G}} - 0.28 \\ \pm 0.41 \quad \pm 0.26 \end{matrix} \quad (10)$$

with an rms scatter in $\log M/L_r$ of 0.097. The relation is shown in Figure 8. The intrinsic scatter is very small, formally 0.035 dex in $\log M/L_r$. We stress that the measurement errors may not be determined accurately enough for this intrinsic scatter to be significant. For the same sample of galaxies the M/L- Mg_2 relation has an rms scatter in $\log M/L_r$ of 0.11 dex and an intrinsic scatter of 0.07 dex. Thus, the improvement in the scatter is small and the coefficient for $\log \text{H}\beta_{\text{G}}$ is significant only on the 2.5σ level. An interesting property of Eq. 10 is that variations in the mean age at a given metallicity will move the data points

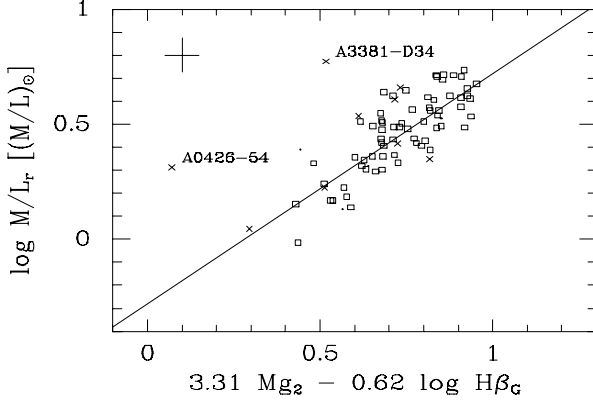


Figure 8. The relation between the M/L ratio and the line indices Mg_2 and $H\beta_G$. Only galaxies in the cluster sample are shown. Symbols as in Fig. 2. Typical error bars are given on the figure. Galaxies with emission lines were not included in the determination of the relation.

nearly parallel to the relation and not contribute significantly to the scatter. This result is based on the models from Vazdekis et al. (1996a), see Table 4. Variations in the metallicity, $[M/H]$, will contribute to the scatter, because a change in $[M/H]$ at a given age gives a three times larger change in $3.31Mg_2 - 0.62 \log H\beta_G$ than in the M/L ratio.

4.5 Other light elements: C and Na

The line index C4668 is a very strong indicator of variations in the carbon abundance (Tripicco & Bell 1995). The line index NaD is mostly sensitive to variations in the sodium abundance. It is also affected by interstellar absorption within the galaxies.

Both C4668 and NaD are correlated with the Mg_2 index and the velocity dispersion, while they are not correlated with the $\langle Fe \rangle$ index. Table 6 lists the derived relations. The relations are shown in Figure 9. The NaD- Mg_2 relation derived here agrees within the uncertainty with the one shown by Burstein et al. (1984).

To the extent that the line indices Mg_2 , C4668 and NaD do measure the abundances of magnesium, carbon and sodium, respectively, the correlations show that the enrichment of E and S0 galaxies with these elements are closely connected. It must await larger samples of galaxies to address if the intrinsic scatter of the relations given in Table 6 is significant, and in that case if it is possible to identify the source of the scatter.

5 PREDICTIONS FROM STELLAR POPULATION MODELS

In this section results from static models of single stellar populations are used to characterize the average properties of the stellar populations in the observed galaxies.

We choose, as our basic set of models, the models from Vazdekis et al. (1996a), which have a bi-modal IMF with

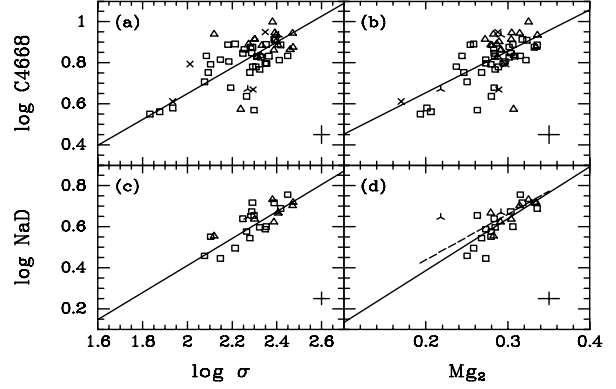


Figure 9. The indices NaD and C4668 versus the velocity dispersion and the Mg_2 index. Symbols as in Fig. 2. Typical error bars are given on the figure. Solid lines – relations given in Table 6. The dashed line on (d) is the relation shown by Burstein et al. (1984).

a Salpeter-like slope of $\mu = 1.35$ and solar abundance ratios. Model ages between 1Gyr and 17Gyr with metallicities of $Z=0.008$, 0.02 and 0.04 are available. The models from Bressan et al. (1996) are consistent with the models from Vazdekis et al. that use a Salpeter IMF, except for the onset of contributions from hot horizontal branch stars for large ages and high metallicities. We supplement the models from Vazdekis et al. with the high metallicity ($Z=0.1$) models from Bressan et al. In order to discuss the abundance ratios in more detail models from Weiss et al. (1995) are used. These authors give models for abundance ratios $[Mg/Fe]$ larger than solar.

None of the conclusions drawn below will change if the basic set of models had been the Worthey (1994) models, or the Vazdekis et al. models with a Salpeter IMF. The models from Buzzoni et al. (1992, 1994) give weaker $\langle Fe \rangle$ and (for $[Fe/H] \geq 0$) stronger $H\beta_G$ for a given age and metallicity, than any of the above mentioned models. The difference originates partly from differences in the adopted fitting functions for the line indices. The models from Buzzoni et al. are not used in the following. Several other stellar population models exist than those mentioned here, see Arimoto (1996) and references herein.

Figure 10 shows the data with the models overplotted. Offsets have been applied to the models from Bressan et al. (1996) such that these authors' model for an age of 15Gyr and $Z=0.02$ would agree with the similar model from Vazdekis et al. The models from Weiss et al. (1995) for $Z=0.02$ have been offset in the same way. The model values for $Z=0.05$ have been derived by linear interpolation between the models for $Z=0.04$ and 0.07 given by Weiss et al., and offset to agreement with the Vazdekis et al. model with an age of 15Gyr and $Z=0.05$. These offsets ensure that the models from Bressan et al. and Weiss et al. can be used together with the Vazdekis et al. models to illustrate the shifts in the observables expected from very high metallicity or non-solar $[Mg/Fe]$.

Figure 11 shows schematically how the observables are expected to change due to variations in age, metallicity,

Table 6. Relations for C4668 and NaD

Relation	N_{gal}	rms	rms _{int}	min.coord.	P
$\log \text{C4668} = (0.63 \pm 0.06) \log \sigma - 0.61$	57	0.092	0.078	perpendicular	< 0.01%
$\log \text{NaD} = (0.66 \pm 0.18) \log \sigma - 0.91$	25	0.053	0.036	perpendicular	< 0.01%
$\log \text{C4668} = (2.02 \pm 0.40) \text{Mg}_2 + 0.25$	57	0.087	0.071	$\log \text{C4668}$	0.02%
$\log \text{NaD} = (2.53 \pm 0.81) \text{Mg}_2 - 0.12$	25	0.069	0.052	$\log \text{NaD}$	< 0.01%

abundance ratio, IMF and fraction of dark matter. The data on this figure include only the galaxies for which all the observables are available.

5.1 Galaxies with strong $H\beta_G$

There is a rather large number of galaxies which have strong Mg_2 (larger than 0.3) and a relatively strong $H\beta_G$, see Figure 10a. The models from Vazdekis et al. (1996a) indicate that these galaxies must have very metal rich stellar populations and also be dominated by very young stars. In fact, nearly half of the galaxies have stronger $H\beta_G$ for their Mg_2 than predicted by any model from Vazdekis et al. The metal rich models from Bressan et al. (1996) are able to predict a strong $H\beta_G$ for galaxies with strong Mg_2 . The strong Balmer line comes from the inclusion of hot horizontal branch stars with high metallicity. However, according to the models these stars only contribute significantly to the strength of the Balmer lines for the very metal rich model ($Z=0.1$).

Changes in the IMF slope give only small differences in the predicted $H\beta_G$ and Mg_2 at a given age and metallicity, see Figure 11a (Vazdekis et al. 1996a). Thus, IMF variations are an unlikely source of the large range of $H\beta_G$. Unless blue horizontal branch stars give a significant contribution to $H\beta_G$ in old galaxies, the large range in $H\beta_G$ cannot easily be explained without a similar substantial range in mean ages.

It also appears that a significant fraction of the galaxies have mean ages smaller than 5Gyr (see also Worthey et al. 1995). This result is, however, very model dependent. It should especially be noted that if the galaxies have an abundance ratio $[\text{Mg}/\text{Fe}]$ above solar then age estimates based on the $H\beta_G$ - Mg_2 diagram and models with $[\text{Mg}/\text{Fe}]=0$ will be too small. Determination of mean ages for the individual galaxies is very uncertain and model dependent, and we will not attempt to do this.

5.2 Abundance ratios

The flat $\langle \text{Fe} \rangle$ - Mg_2 relation is not predicted by the stellar population models (Figure 10b). This result does not depend on the assumed IMF. The only known effect that can lead to a nearly constant $\langle \text{Fe} \rangle$ while Mg_2 varies from 0.2 to 0.34 is non-solar abundance ratios, see Figure 11b. Thus, the data and the models restate the result by Worthey et al. (1992), that for E and S0 galaxies with strong magnesium lines the abundance ratio $[\text{Mg}/\text{Fe}]$ is larger than solar. The two models from Weiss et al. (1995), which we have shown on Figure 10, have $[\text{Mg}/\text{Fe}]=0.4$ and a total metallicity of $Z=0.02$ and $Z=0.05$, respectively. The abundance ratio $[\text{Mg}/\text{Fe}]$ is varied by changing the mix of elements while keeping the total metallicity constant. Changing $[\text{Mg}/\text{Fe}]$ from zero to 0.4 means that the iron abundance is decreased with a factor

2.1, while the magnesium abundance is increased with a factor 1.2. Thus, the model with $Z=0.02$ has $[\text{Fe}/\text{H}]=-0.32$ and $[\text{Mg}/\text{H}]=0.08$, and the model with $Z=0.05$ has $[\text{Fe}/\text{H}]=0.08$ and $[\text{Mg}/\text{H}]=0.48$.

It is clear from the models that in order to get Mg_2 larger than 0.29 the magnesium abundance needs to be above solar. In the presence of non-solar abundance ratios a total metallicity above solar is only needed for those galaxies that also have a relatively strong iron index ($\log \langle \text{Fe} \rangle > 0.5$). We conclude that for solar metallicity ($Z=0.02$) the galaxies with Mg_2 larger than 0.29 must have $[\text{Mg}/\text{Fe}]$ between zero and 0.6, a typical value being 0.3. Galaxies with both strong Mg_2 (larger than 0.32) and strong $\log \langle \text{Fe} \rangle$ (larger than 0.5) are best fit with models that have above solar metallicity ($Z=0.05$) and $[\text{Mg}/\text{Fe}]$ around 0.4. These estimates are in general agreement with results from Worthey et al. (1992) and Weiss et al. (1995). Finally, about half the galaxies with Mg_2 in the interval between 0.2 and 0.29 can be fit with above solar metallicity and solar abundance ratios, while the other half must have $[\text{Mg}/\text{Fe}] > 0$.

5.3 The M/L ratio, the IMF, and the fraction of dark matter

Changes in the age or the metallicity of a stellar population naturally lead to changes in the M/L ratio, see Figure 10c-e. A change in the slope of the IMF gives a strong change in the M/L ratio. For the models with ages larger than 5Gyr and a bi-modal IMF an increase in the slope from $\mu = 1.35$ to $\mu = 2.35$ results in a change in $\log \text{M/L}$ of +0.2 (see Figure 11c-e). The changes for the models with ages 5Gyr or younger are even larger. For all the models it is, however, expected that the M/L ratio and $H\beta_G$ are strongly correlated, independent of age and metallicity.

In Sect. 4.1 we found that the relation between $\log \text{M/L}$ and $\log H\beta_G$ has significant intrinsic scatter, 0.1 in $\log \text{M/L}$. The relation has nearly the same slope as expected if all the galaxies have stellar populations with the same IMF. The scatter cannot easily be explained as due to differences in age and/or metallicity. An increase in the abundance ratio $[\text{Mg}/\text{Fe}]$ may lead to a decrease in $H\beta_G$ (cf. Tripicco & Bell 1995). If variations in the abundance ratios at a given M/L ratio cause the scatter in the relation between the M/L ratio and $H\beta_G$ then it is expected that the residuals for this relation are correlated with the residuals for the M/L- Mg_2 relation and either anti-correlated or uncorrelated with the residuals for the M/L- $\langle \text{Fe} \rangle$ relation. However, the residuals for all three relations are correlated with each other, and the slopes of these correlations are close to one. Thus, it does not seem likely that variations in the abundance ratio $[\text{Mg}/\text{Fe}]$ can cause the scatter in the M/L- $H\beta_G$ relation. We are left with two other possibilities. Either (1) the IMF of the current stellar population in the galaxies varies from galaxy

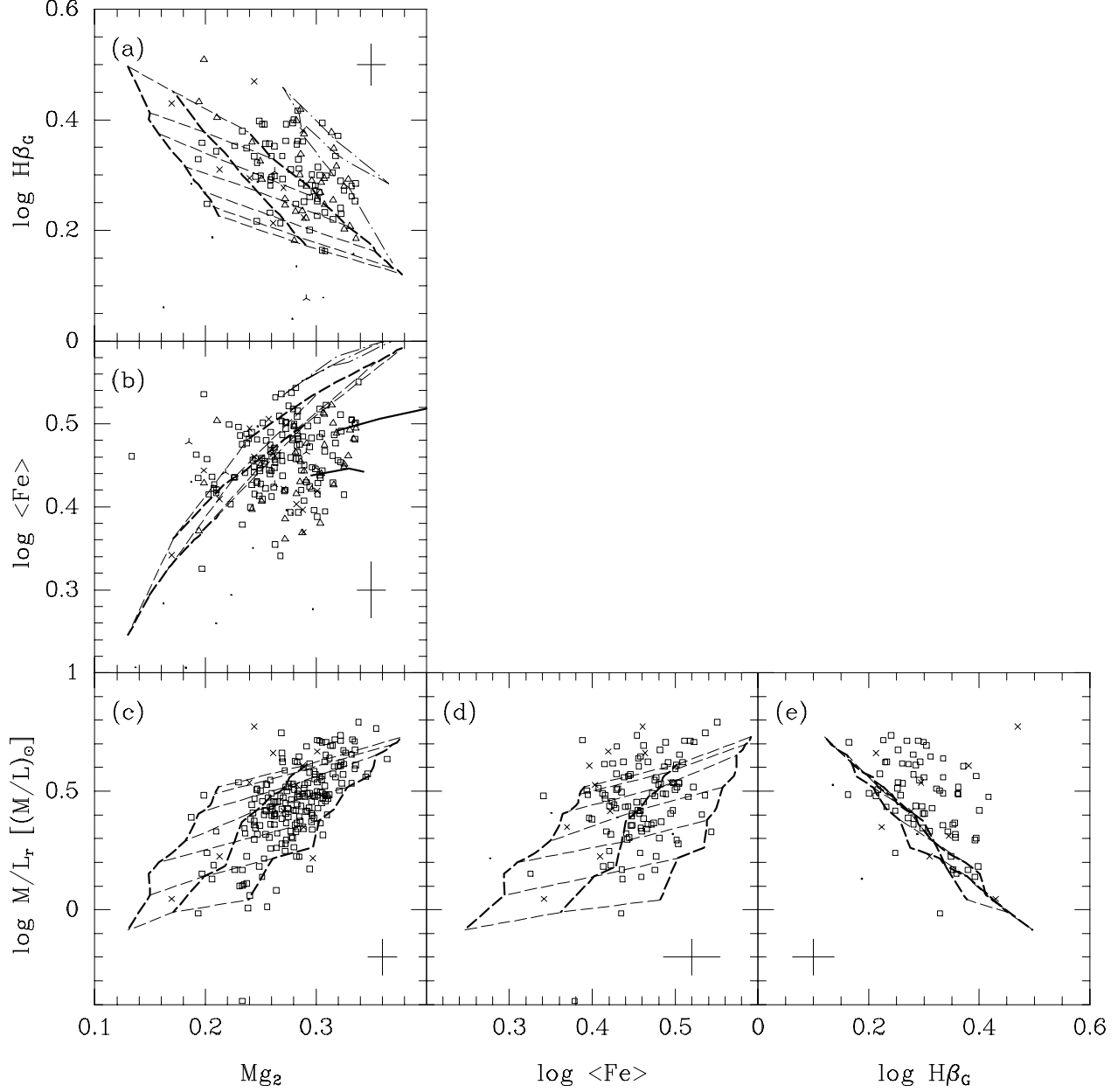


Figure 10. The line indices (Mg_2 , $H\beta_G$ and $\langle Fe \rangle$) and the M/L ratio versus each other. Data symbols as in Figure 2. Typical error bars are given on the panels. Predictions from static stellar population models are overplotted. Dashed lines – Vazdekis et al. (1996a), thick lines are constant metallicity ($Z=0.008, 0.02, 0.05$), thin lines are constant age (2, 3, 5, 8, 12, 15, and 17 Gyr). Dot-dashed lines – Bressan et al. (1996), $Z=0.1$, ages from 2Gyr to 17Gyr. Solid lines – Weiss et al. (1995) with $[Mg/Fe]=0.4$ ($Z=0.02$ and 0.05 , ages from 12Gyr to 18Gyr).

to galaxy, in the sense that galaxies with higher than usual M/L ratio have a steeper IMF, and galaxies with lower than usual M/L ratio have a shallower IMF. Or (2) the fraction of dark matter in the galaxies varies. For both effects it is expected that the residuals for the three relations between the M/L ratios and the line indices are correlated with a slope close to one. This is in agreement with the data. A larger sample of galaxies with $H\beta_G$ measured with a bet-

ter accuracy than for the present data is needed to address the significance of the intrinsic scatter in the M/L ratio at a given $H\beta_G$. It is not clear, however, that it will be possible to distinguish between the two possible reasons for the scatter outlined above.

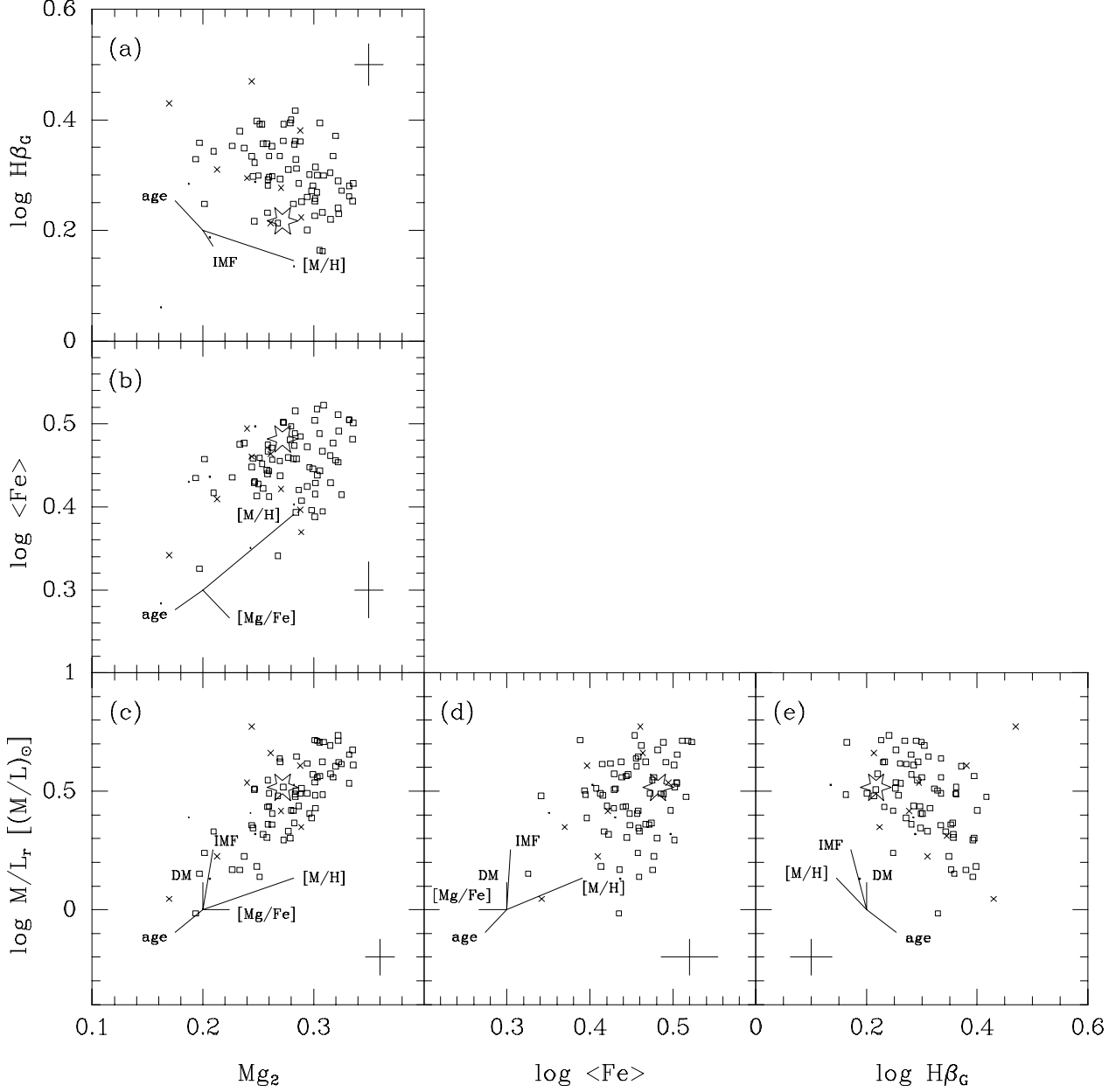


Figure 11. The line indices (Mg_2 , $H\beta_G$ and $\langle Fe \rangle$) and the M/L ratio versus each other. Only galaxies in the cluster sample for which we have all parameters are plotted, a total of 84 galaxies. Data symbols as in Figure 2. Typical error bars are given on the panels. Large stars – model values from Vazdekis et al. (1996a) for $[M/H]=0$, $[Mg/Fe]=0$, age=12Gyr, and slope of the bi-modal IMF $\mu = 1.35$. The lines indicate expected changes in the observables due to changes in $[M/H]$, $[Mg/Fe]$, age, IMF slope and fraction of dark matter, see Sect. 5.4. Note that the indicated change in age is towards younger models.

5.4 The general trends

The diagrams of the M/L ratio versus Mg_2 , $\log \langle Fe \rangle$, and $\log H\beta_G$ can together with the indices plotted versus each other be used as a diagnosis for which effects govern the evolution of the E and S0 galaxies. This is illustrated in Figure 11, which shows the galaxies in the cluster sample for which all the required parameters are available. The large star symbols on the panels mark the model values from Vazdekis et

al. (1996a) for solar metallicity and abundance ratios, an age of 12 Gyr, and bi-modal IMF with slope $\mu = 1.35$. Based on the same models the lines on the panels show how changes in total metallicity $[M/H]$, abundance ratio $[Mg/Fe]$, mean age, mean IMF, and fraction of dark matter will affect the parameters. The length of the lines show changes in $[M/H]$ and $[Mg/Fe]$ from 0.0 to 0.4 at age 12Gyr and IMF slope $\mu = 1.35$, in ages from 12Gyr to 8Gyr at solar metallicity and

IMF slope $\mu = 1.35$, and in slope of the IMF from $\mu = 1.35$ to $\mu = 2.35$ at age 12Gyr and solar metallicity. The change in fraction of dark matter is shown as the change from adding 30% mass to the galaxy in the form of dark matter. The origin of the lines has been arbitrarily shifted from the location of the star symbols in order to avoid conflict with the data points.

Ideally we want to derive from the observables (Mg_2 , $\langle Fe \rangle$, $H\beta_G$, M/L) the physical parameters ($[M/H]$, $[Mg/Fe]$, age, IMF, fraction of dark matter). Age, IMF and abundances should be understood as luminosity weighted mean parameters for the stellar populations presently observed. There are five independent physical parameters and only four observables, excluding any environment parameters. However, if the fraction of dark matter is not superimposed by initial conditions during the formation of the galaxy, but is related to the evolution of the galaxies in a way that links it to the abundance ratios (specifically $[Mg/Fe]$) then it may be possible to derive the physical parameters from the four observables.

It has been suggested that the abundance ratio $[Mg/Fe]$ above solar is related to the presence of a short period of star formation early on with an IMF heavily biased towards high mass stars (Vazdekis et al. 1996a; Worthey et al. 1992). Vazdekis et al. fit observational data for three nearby E galaxies with models that have a period of ≈ 1 Gyr where the IMF has a rather flat slope, followed by an evolution with an IMF with a steeper slope. No M/L ratios are given for these models. However, if we assume a conservative average remnant mass of $1M_\odot$ for all stars with initial mass larger than $2M_\odot$ then a flat IMF with lower and upper cut-off as used by Vazdekis et al. in the first 1Gyr of a galaxy's evolution will turn some 10% of the mass into stellar remnants. Assuming these remnants at the present age do not contribute significantly to the luminosity the M/L ratio increases with a similar amount relative to a model with the same steep IMF during the whole evolution. A more stringent test of the idea outlined here requires that evolutionary models like those by Vazdekis et al. (1996a) include predictions of the evolution of the M/L ratio.

6 DISCUSSION AND CONCLUSIONS

We have investigated the stellar populations in E and S0 galaxies based on spectral line index data for a large sample of cluster E and S0 galaxies. The line indices are on the Lick/IDS system, except the index for the $H\beta$ line which has been redefined to give a better signal-to-noise. The indices Mg_2 , $\langle Fe \rangle$ and $H\beta_G$ are used as the primary indices to characterize the stellar populations.

Relations were established between the indices and the velocity dispersion, the mass, and the M/L ratio of the galaxies. The relations were used to study which effects determine the current stellar populations. Also, the influence of the environment has been studied. It is tested whether the M/L ratio depends only on the stellar populations. The E and the S0 galaxies follow the same relations. In the following discussion the E and S0 galaxies are, therefore, treated as one class of galaxies. This does not exclude that there are substantial variations in the relative disk luminosities (e.g., Jørgensen & Franx 1994).

We assume that Mg_2 and $\langle Fe \rangle$ for a galaxy with a given mean age are related to the magnesium abundance and the iron abundance, respectively. Both indices are also sensitive to the age, and $\langle Fe \rangle$ reacts as much to a change in the total metallicity as to a change in the iron abundance. The $H\beta_G$ is sensitive to the mean age, but also to the relative contribution from blue horizontal stars and to the metallicity.

The Mg_2 index is strongly correlated with the velocity dispersion and the mass of the galaxies. The Mg_2 - σ relation for E galaxies has long been well-established (Burstein et al. 1988b; Bender et al. 1993). There are galaxies with strong $H\beta_G$ which have weak Mg_2 for their velocity dispersion. Further, Mg_2 is weakened if the galaxy has emission lines. Both these effects can be understood if the strong $H\beta_G$ and/or emission are due to a young stellar population. This possibility for galaxies with weak Mg_2 was mentioned already by Burstein et al. (1988b). The galaxies with emission lines also have weak $\langle Fe \rangle$ as would be expected. However, some galaxies with strong $H\beta_G$ and weak Mg_2 have fairly normal $\langle Fe \rangle$. It is not clear why this is the case, and it may indicate that something important is missing in our interpretation of these indices.

The residuals for the Mg_2 - σ relation depend on the environment, specifically $\rho_{\text{cluster}} = \sigma_{\text{cluster}}^2/R$, which is a measure of the projected surface density of the cluster. R is the cluster center distance. Galaxies in low density environments tend to have slightly weaker Mg_2 for their velocity dispersion than galaxies in high density environments. However, the dependence on ρ_{cluster} explains only a very small fraction of the intrinsic scatter in the Mg_2 - σ relation.

The $\langle Fe \rangle$ index is weakly correlated with the velocity dispersion and the mass of the galaxies. However, for galaxies with velocity dispersion between 100km s^{-1} and 250km s^{-1} the $\langle Fe \rangle$ index shows no significant correlations with the velocity dispersion or the mass. The $\langle Fe \rangle$ index correlates weakly with the Mg_2 index, and is uncorrelated with $H\beta_G$ index. The $\langle Fe \rangle$ index is stronger correlated with ρ_{cluster} than with the mass and the velocity dispersion of the galaxy. Galaxies in low density environments have in general smaller $\langle Fe \rangle$ than galaxies in high density environments.

The $H\beta_G$ index is correlated with the velocity dispersion, the mass, and the Mg_2 index. The index itself as well as the residuals for the various relations are not significantly correlated with the cluster environment.

The M/L ratio is strongly correlated with the Mg_2 index and the $H\beta_G$ index, while the correlation with the $\langle Fe \rangle$ index is very weak. A relation between the M/L ratio, Mg_2 and $H\beta_G$ has a very low intrinsic scatter.

The data were compared to single stellar population models from Vazdekis et al. (1996a). There are three main points from this comparison. (1) Galaxies with strong $H\beta_G$ and strong Mg_2 require either very metal rich and young stellar populations, or a significant contribution to $H\beta_G$ from blue horizontal stars. (2) The flat $\langle Fe \rangle$ - Mg_2 relation restates the result by Worthey et al. (1992) that many of the strong lined E and S0 galaxies must have abundance ratios $[Mg/Fe]$ larger than solar. (3) The intrinsic scatter in the $H\beta_G$ - M/L relation is not predicted by the models unless there are variations in the IMF and/or the fraction of dark matter in the galaxies.

The two first points may be resolved and quantified when better stellar population models become available. The third point, however, cannot easily be resolved. The difficulty is how to distinguish between IMF differences and variations in the fraction of dark matter. If the fraction of dark matter is mostly determined by the formation process of the galaxy, it may not be possible to break this degeneracy. If on the other hand the fraction of dark matter is a natural consequence of the evolution of the galaxy it may be possible to identify the source of the scatter.

Based on the results summarized above it seems clear that different processes must affect the magnesium index and the iron index, and maybe also the abundances of these two elements. We will here discuss this in a little more detail.

Variations in the mean age of the stellar populations are expected to change Mg_2 and $\log \langle Fe \rangle$ with the same amounts. The shallow slope of the $\langle Fe \rangle$ - σ relation compared to the Mg_2 - σ relation, therefore, shows that the abundance ratio $[Mg/Fe]$ changes with velocity dispersion. We estimate that the $[Mg/Fe]$ for galaxies with velocity dispersions of 250 km s^{-1} is 0.3 to 0.4 dex larger than for galaxies with velocity dispersions of 100 km s^{-1} . If the galaxies are coeval the difference is due to an increase in the magnesium abundance. Otherwise it is (partly) due to a decrease in the iron abundance. The $H\beta_G$ index may offer a possibility to distinguish between the two possibilities, if this index can be used to trace age variations. However, most of the current models cannot reproduce the strong $H\beta_G$ seen in some galaxies with strong Mg_2 . It is also not known how $H\beta_G$ reacts to changes in $[Mg/Fe]$, though results from Tripicco & Bell (1995) indicate that most of the change in $H\beta_G$ due to changes in the metallicity is caused by the magnesium abundance. Thus, better models may be needed before this technique will be feasible.

There are several studies in the literature that indicate that the stellar populations of E and S0 galaxies are influenced by the environment (Guzmán et al. 1992; de Carvalho & Djorgovski 1992; Rose et al. 1994). The dependence of the $\langle Fe \rangle$ index and the Mg_2 index on the environment we find from our analysis implies that $[Mg/Fe]$ is approximately 0.1 dex lower in high density environments ($\log \rho_{\text{cluster}}=7$) compared to low density environments ($\log \rho_{\text{cluster}}=4.5$). Independent of possible age differences, the decrease is caused by the iron abundance increasing faster with the cluster density, than the (possible) increase in the magnesium abundance with cluster density.

We note, that literature data show that the Mg_2 index and the $\langle Fe \rangle$ index both change within the galaxies. The average radial gradients of the two indices are consistent with a rather small $[Mg/Fe]$ variation within each galaxy (Worthey et al. 1992; Davies et al. 1993; Fisher et al. 1995, 1996).

The detection of variations in $[Mg/Fe]$ leaves us with the challenge of explaining the cause of the variations among the galaxies and the nearly constant $[Mg/Fe]$ within each galaxy. Three possible explanations for above solar $[Mg/Fe]$ have been mentioned and to some extent explored by Worthey et al. (1992) and Matteucci (1994). Different time scales for star formation, different IMFs, and selective galactic wind loss of metals. These authors have not addressed the possible effect of the cluster environment. The environment dependence of $[Mg/Fe]$ found in this paper is about a third of the

size of the change related to the velocity dispersion of the galaxies. Thus, it may be important for our understanding of the abundance ratios that environment effects are taken into account.

Acknowledgements: This paper benefited from discussions with M. Franx. S. M. Faber is thanked for making unpublished data available from the Lick project on spectral line indices for elliptical galaxies. G. Worthey and R. Peletier are thanked for supplying their stellar population models in computer readable format. The Danish Board for Astronomical Research and the European Southern Observatory are acknowledged for assigning observing time for this project and for financial support. This research was supported through Hubble Fellowship grant number HF-01073.01.94A from the Space Telescope Science Institute, which is operated by the Association of Universities for Research in Astronomy, Inc., under NASA contract NAS5-26555.

REFERENCES

- Aaronson, M., Cohen, J. G., Mould, J., Malkan, M. 1978, *ApJ*, 223, 824
- Arimoto, N. 1996, in *From Stars to Galaxies*, eds. Leitherer, C., Frize-von Alvensleben, U., Huchra, J., ASP Conf. Ser. Vol 98, Astron. Soc. Pac., San Francisco, p. 287
- Baade, W. 1944, *ApJ*, 100, 137
- Bender, R., Burstein, D., Faber, S. M. 1993, *ApJ*, 411, 153
- Bressan, A., Chiosi, C., Tantalo, R. 1996, *A&A*, 311, 425
- Bruzual, A. G. 1983, *ApJ*, 273, 105
- Bruzual, A. G., Charlot, S. 1993, *ApJ*, 405, 538
- Burstein, D., Bertola, F., Buson, L. M., Faber, S. M., Lauer, T. R. 1988a, *ApJ*, 328, 440
- Burstein, D., Davies, R. L., Dressler, A., Faber, S. M., Lynden-Bell, D., Terlevich, R. J., Wegner, G. 1988b, in *Towards Understanding Galaxies at Large Redshifts*, eds. Kron, R. G., Renzini, A., (Dordrecht: Kluwer), 17
- Burstein, D., Faber, S. M., Dressler, A. 1990, *ApJ*, 354, 18
- Burstein, D., Faber, S. M., Gaskell, C. M., Krumm, N. 1984, *ApJ*, 287, 586
- Buzzoni, A. 1989, *ApJS*, 71, 817
- Buzzoni, A. 1995, *ApJS*, 98, 69
- Buzzoni, A., Giraboldi, G., Mantegazza, L. 1992, *AJ*, 103, 1814
- Buzzoni, A., Mantegazza, L., Giraboldi, G. 1994, *AJ*, 107, 513
- Caldwell, N., Rose, J. A., Sharples, R. M., Ellis, R. S., Bower, R. 1993, *AJ*, 106, 473
- Carollo, C., Danziger, I. J., Buson, L. 1993, *MNRAS*, 265, 553
- Charlot, S., Worthey, G., Bressan, A. 1996, *ApJ*, 457, 625
- Davidge, T. J. 1992, *AJ*, 103, 1512
- Davies, R. L., Burstein, D., Dressler, A., Faber, S. M., Lynden-Bell, D., Terlevich, R. J., Wegner, G. 1987, *ApJS*, 64, 581
- Davies, R. L., Sadler, E. M., Peletier, R. F. 1993, *MNRAS*, 262, 650
- de Carvalho, R. R., Djorgovski, S. 1992, *ApJ*, 389, L49
- Dressler, A. 1987, *ApJ*, 317, 1
- Faber, S. M. 1994, private communication
- Faber, S. M., Friel, E. D., Burstein, D., Gaskell, C. M. 1985, *ApJS*, 57, 711
- Faber, S. M., Wegner, G., Burstein, D., Davies, R. L., Dressler, A., Lynden-Bell, D., Terlevich, R. J. 1989, *ApJS*, 69, 763
- Fisher, D., Franx, M., Illingworth, G. 1995, *ApJ*, 448, 119
- Fisher, D., Franx, M., Illingworth, G. 1996, *ApJ*, 459, 110
- Franx, M., Illingworth, G., Heckman, T. 1989, *ApJ*, 344, 613
- González, J. J. 1993, Ph.D. thesis, Univ. of California, Santa Cruz

- Gorgas, J., Efstathiou, G., Aragón-Salamanca, A. 1990, MNRAS, 245, 217
- Goudfrooij, P., Emsellem, E. 1996, A&A, 306, L45
- Goudfrooij, P., Hansen, L., Jørgensen, H. E., Nørgaard-Nielsen, H. U. 1994, A&AS, 105, 341
- Guzmán, R., Lucey, J. R., Carter, D., Terlevich, R. J. 1992, MNRAS, 257, 187
- Hickson, P. 1982, ApJ, 255, 382
- Hickson, P., Mendes de Oliveira, C., Huchra, J. P., Palumbo, G. G. C. 1992, ApJ, 399, 353
- Jones, L. A., Worthey, G. 1995, ApJ, 446, L31
- Jørgensen, I., Franx, M. 1994, ApJ, 433, 553
- Jørgensen, I., Franx, M., Kjaergaard, P. 1995a, MNRAS, 273, 1097
- Jørgensen, I., Franx, M., Kjaergaard, P. 1995b, MNRAS, 276, 1341 (Paper I)
- Jørgensen, I., Franx, M., Kjaergaard, P. 1996, MNRAS, 280, 167 (Paper II)
- Lucey, J. R., Guzmán, R., Carter, D., Terlevich, R. J. 1991b, MNRAS, 253, 584
- Maia, M. A. G., da Costa, L. N., Latham, D. W. 1989, ApJS, 69, 809
- Matteucci, F. 1994, A&A, 288, 57
- Peletier, R. F. 1989, PhD Thesis, University of Groningen
- Peletier, R. F., Balcells, M. 1996, AJ, 111, 2238
- Renzini, A., Ciotti, L. 1993, ApJ, 416, L49
- Rose, J. A., Bower, R. G., Caldwell, N., Ellis, R. S., Sharples, R. M., Teague, P. 1994, AJ, 108, 2054
- Salpeter, E. E. 1955, ApJ, 121, 161
- Silva, D., Elston, R. 1994, ApJ, 428, 511
- Tinsley, B. M., Gunn, J. E. 1976, ApJ, 206, 525
- Tripcic, M. J., Bell, R. A. 1995, AJ, 110, 3035
- van der Waerden, B. L. 1969, Mathematical Statistics (Berlin: Springer Verlag)
- Vazdekis, A., Casuso, E., Peletier, R. F., Beckman, J. E. 1996a, ApJS, 106, 307
- Vazdekis, A., Casuso, E., Peletier, R. F., Beckman, J. E. 1996b, preprint
- Weiss, A., Peletier, R. F., Matteucci, F. 1995, A&A, 296, 73
- Worthey, G. 1994, ApJS, 95, 107
- Worthey, G., Faber, S. M., González, J. J., 1992, ApJ, 398, 69
- Worthey, G., Faber, S. M., González, J. J., Burstein, D. 1994, ApJS, 94, 687
- Worthey, G., Trager, S. C., Faber, S. M. 1995, in Fresh Views on Elliptical Galaxies, eds. Buzzoni, A., Renzini, A., Serrano, A., ASP Conf. Ser. Vol. 86, Astron. Soc. Pac., San Francisco, p. 203

APPENDIX A: SPECTROSCOPIC DATA

The spectra used in this paper were obtained during three observing runs at the ESO 1.5m telescope with the B&C spectrograph and one observing run at the ESO 3.6m telescope with the OPTOPUS instrument. Information about the instrumentation and the basic reductions can be found in Paper I.

A1 Determination of line indices

The line indices were derived from the flux calibrated spectra convolved to the Lick/IDS instrumental dispersion ($\sigma = 200 \text{ km s}^{-1}$, González 1993). The B&C spectra were averaged within the apertures given in Paper I (B&C run 1 and run 2 $2''.5 \times 8''.16$; B&C run 3 $2''.5 \times 6''.8$). The wavelength intervals for the indices are given by Worthey et al. (1994) and in Table 2. All indices except Mg_1 and Mg_2 were derived as the

equivalent width. Mg_1 and Mg_2 are given as a magnitude (see also Worthey et al.).

The average values corrected for the aperture size and for the effect of the velocity dispersion are listed in Tables A1 and A2. For convenience also the velocity dispersion and the Mg_2 index as published in Paper I are included in Table A1.

A2 Aperture corrections

Because E and S0 galaxies have radial gradients in most line indices the derived 'central' values depend on the distances of the galaxies and the size of the aperture. The indices have to be corrected to a standard size aperture. A circular aperture with diameter $1.19h^{-1}$ kpc was adopted as the standard size. This is equivalent to 3.4 arcsec at the distance of the Coma cluster.

In general the radial gradients are well described as logarithmic gradients $\Delta \log(\text{index})/\Delta \log r$. For Mg_1 and Mg_2 $\Delta \text{Mg}_i/\Delta \log r$ gives a better description, cf. Fisher et al. (1995, 1996). The radial gradient in the velocity dispersion can also be described as a logarithmic gradient (e.g. Franx, Illingworth & Heckman 1989). We therefore assume that the aperture corrections for the line indices can be written in the same form as for the velocity dispersion. We use

$$\log(\text{index})_{\text{norm}} = \log(\text{index})_{\text{ap}} + \alpha \log \frac{r_{\text{ap}}}{r_{\text{norm}}} \quad (\text{A1})$$

except for Mg_1 and Mg_2 , where we use

$$(\text{index})_{\text{norm}} = (\text{index})_{\text{ap}} + \alpha \log \frac{r_{\text{ap}}}{r_{\text{norm}}} \quad (\text{A2})$$

cf. Paper I. $\alpha(\text{Mg}_2) = \alpha(\text{Mg}_1) = 0.04$ was used (Paper I).

González (1993) has derived line indices within apertures with radii $r_e/8$ and $r_e/2$ for 41 galaxies. r_e is the effective radius of the galaxy. From the average values we find that $\alpha(\text{Mgb}) \cong \alpha(<\text{Fe}>) \cong 0.05$ and $\alpha(\text{H}\beta) \cong -0.005$. We also adopt $\alpha = 0.05$ for all other Fe indices. Fisher et al. (1995, 1996) find the gradients for C4668 (called Fe4668 by these authors) to be somewhat stronger than for Mgb, Fe5270 and Fe5335. Mean of all their determinations gives $\Delta \log(\text{index})/\Delta \log r = -0.11$ for C4668, while the values for Mgb, Fe5270 and Fe5335 are -0.063 , -0.054 and -0.051 , respectively. We therefore adopt $\alpha(\text{C4668}) = 0.08$.

Vazdekis et al. (1996) have measured radial gradients of line indices for 3 galaxies. Their study includes NaD. They give gradients as $\Delta(\text{index})/\Delta \log r$, and find the gradient for NaD to be significantly stronger than for Mgb, Fe5270 and Fe5335. Mean for the three galaxies gives -1.53 for NaD. The mean gradients for Mgb, Fe5270 and Fe5335 are -0.88 , -0.55 and -0.50 , respectively. The strength of NaD is in general comparable to Mgb, while the iron lines are weaker. We adopt $\alpha(\text{NaD}) = 0.09$.

A3 Correction for the velocity dispersion

All the derived line indices, except H β in emission, were corrected for the effect of the velocity dispersion. The corrections were established from K-giant spectra. The star spectra were convolved to the Lick/IDS instrumental resolution, and then convolved with Gaussians with σ from 50 to 350 km s^{-1} . For Mg_1 the differences between the index from the

TABLE A1
SPECTROSCOPIC PARAMETERS, MEAN VALUES

Galaxy	$\log \sigma$	C4668	H β	H β_{G}	Fe5015	Mg ₁	Mg ₂	Mgb	< Fe >	Fe5406
A194:										
D52	1.876	3.64	1.29	1.54	5.44	0.083	0.206	3.15	2.73	1.89
	0.041	0.90	0.37	0.25	0.73	0.009	0.011	0.39	0.34	0.40
I0120	2.040	...	1.81	1.94	3.29	0.092	0.247	3.76	3.14	1.55
	0.053	...	0.55	0.37	1.11	0.013	0.017	0.58	0.51	0.60
I1696	2.186	6.41	1.68	2.00	5.24	0.133	0.296	4.27	2.80	1.78
	0.022	0.57	0.24	0.16	0.47	0.006	0.007	0.25	0.22	0.26
N0533	2.412	6.51	1.73	1.74	4.51	0.157	0.322	4.92	2.84	2.19
	0.032	0.86	0.36	0.25	0.72	0.009	0.011	0.37	0.34	0.39
N0535 ^b	2.111	...	2.26	2.38	4.67	0.094	0.242	3.78	2.93	1.71
	0.046	...	0.48	0.33	0.98	0.012	0.015	0.52	0.46	0.54
N0541	2.283	7.52	1.97	1.79	4.21	0.154	0.301	4.52	3.19	1.41
	0.030	0.73	0.31	0.21	0.62	0.008	0.009	0.32	0.29	0.34
N0545	2.364	6.79	1.43	1.71	4.99	0.145	0.308	4.75	2.93	1.83
	0.014	0.53	0.16	0.11	0.32	0.004	0.005	0.17	0.15	0.18
N0547	2.394	8.13	1.44	1.70	5.02	0.159	0.323	5.07	3.10	1.76
	0.013	0.35	0.15	0.10	0.30	0.004	0.005	0.15	0.14	0.16
N0548	2.092	5.66	1.17	1.65	4.67	0.097	0.246	4.20	2.69	1.74
	0.035	0.76	0.32	0.22	0.63	0.008	0.010	0.33	0.30	0.35
N0560	2.254	7.32	2.12	2.27	5.84	0.128	0.283	4.36	2.98	1.73
	0.015	0.43	0.18	0.12	0.36	0.004	0.005	0.19	0.17	0.20
N0564	2.355	6.27	1.47	1.82	4.74	0.143	0.294	4.58	2.66	1.87
	0.022	0.52	0.22	0.15	0.44	0.005	0.007	0.23	0.21	0.24
ZH07	2.181	7.72	2.19	2.27	5.20	0.111	0.254	4.30	2.64	1.67
	0.026	0.68	0.28	0.19	0.57	0.007	0.009	0.30	0.27	0.31
ZH09	2.085	6.82	1.96	2.16	4.71	0.092	0.244	3.90	2.81	1.75
	0.026	0.60	0.25	0.17	0.50	0.006	0.008	0.26	0.23	0.27
ZH10	2.321	...	1.43	1.66	4.10	0.139	0.315	5.24	2.69	1.81
	0.027	...	0.32	0.22	0.65	0.008	0.010	0.33	0.30	0.35
ZH12	2.211	...	1.35	1.71	5.49	0.110	0.259	3.85	2.75	1.81
	0.019	...	0.22	0.15	0.43	0.005	0.007	0.23	0.20	0.24
ZH19	2.052	...	2.21	2.40	5.04	0.093	0.233	4.54	2.99	2.04
	0.025	...	0.24	0.16	0.49	0.006	0.007	0.25	0.23	0.26
ZH31	1.833	3.55	2.03	2.13	4.82	0.070	0.193	3.11	2.72	1.19
	0.037	0.74	0.30	0.20	0.60	0.007	0.009	0.32	0.28	0.33
ZH39	2.280	...	1.69	1.96	4.53	0.117	0.270	4.57	2.74	1.70
	0.019	...	0.20	0.13	0.40	0.005	0.006	0.20	0.19	0.22
ZH52 ^c	2.011	6.21	-0.46	-0.41	3.17	0.138	0.297	4.94	1.89	1.79
	0.043	0.79	0.35	0.24	0.67	0.008	0.010	0.34	0.32	0.36
ZH53	1.934	3.80	1.37	1.77	4.15	0.078	0.201	3.63	2.87	1.42
	0.039	0.87	0.36	0.24	0.71	0.009	0.010	0.37	0.33	0.39
ZH56 ^a	2.328	6.82	1.71	1.97	4.59	0.141	0.308	4.63	2.98	1.65
	0.018	0.47	0.20	0.13	0.39	0.005	0.006	0.20	0.18	0.22
A539:										
D16 ^c	2.295	4.67	1.39	1.67	3.17	0.139	0.289	4.54	2.34	...
	0.030	0.84	0.34	0.23	0.70	0.008	0.010	0.36	0.33	...
D22 ^a	2.134	...	2.43	2.71	5.00	0.086	0.194	3.31	2.35	...
	0.034	...	0.27	0.18	0.54	0.007	0.008	0.29	0.26	...
D23 ^a	2.074	...	2.09	2.54	3.09	0.104	0.210	1.79	3.19	...
	0.064	...	0.46	0.31	0.94	0.011	0.014	0.51	0.43	...
D29	2.118	6.06	0.098	0.252	3.97	2.57	2.40
	0.040	0.61	0.008	0.009	0.32	0.29	0.33
D31	2.200	5.61	0.109	0.242	3.90	2.67	1.97
	0.021	0.41	0.005	0.006	0.22	0.19	0.22
D35	2.284	6.51	0.156	0.289	4.91	2.82	1.90
	0.022	0.44	0.006	0.007	0.23	0.21	0.24
D36	2.087	5.87	0.121	0.278	4.31	3.45	1.90
	0.031	0.57	0.007	0.009	0.30	0.27	0.32
D37	2.251	6.64	0.118	0.284	4.29	3.06	1.92
	0.017	0.36	0.004	0.006	0.19	0.17	0.20
D38 ^b	2.238	6.52	0.121	0.269	4.16	3.15	2.27
	0.022	0.43	0.005	0.007	0.23	0.20	0.24
D39	2.226	4.83	0.122	0.263	4.20	2.84	1.75
	0.018	0.35	0.004	0.005	0.18	0.17	0.19
D41	2.203	6.02	0.117	0.262	4.14	2.80	2.38
	0.025	0.44	0.006	0.007	0.24	0.21	0.24
D42	2.176	4.73	0.116	0.265	4.34	2.89	1.92
	0.022	0.45	0.006	0.007	0.23	0.21	0.24
D43	2.091	4.48	0.081	0.199	3.38	3.43	1.51
	0.029	0.56	0.007	0.008	0.30	0.26	0.31
D44	2.298	5.95	0.133	0.273	4.52	3.12	2.23
	0.013	0.29	0.004	0.004	0.15	0.14	0.16
D45	2.354	5.22	0.161	0.316	5.18	3.07	2.48
	0.015	0.31	0.004	0.005	0.16	0.15	0.17
D48	2.269	5.30	0.143	0.296	5.12	3.04	1.53
	0.019	0.37	0.005	0.006	0.19	0.18	0.21

TABLE A1—*Continued*

Galaxy	$\log \sigma$	C4668	H β	H β_G	Fe5015	Mg ₁	Mg ₂	Mgb	< Fe >	Fe5406
D50	2.355	3.72	0.135	0.293	4.56	3.14	1.80
	0.017	0.35	0.004	0.005	0.18	0.16	0.19
D51	2.221	5.62	0.117	0.263	4.37	3.40	2.10
	0.018	0.37	0.005	0.006	0.19	0.17	0.20
D52	2.145	6.17	0.127	0.269	3.66	2.90	2.35
	0.030	0.51	0.006	0.008	0.28	0.24	0.28
D53	2.384	3.45	0.114	0.275	5.06	3.33	1.89
	0.016	0.36	0.004	0.005	0.18	0.16	0.19
D54	2.138	5.60	0.124	0.255	4.34	3.02	2.00
	0.024	0.48	0.006	0.007	0.25	0.23	0.26
D57 ^c	2.247	2.29	0.151	0.301	5.32	2.63	1.51
	0.024	0.44	0.005	0.007	0.22	0.20	0.24
D59	2.232	6.32	0.123	0.279	5.01	3.04	1.84
	0.023	0.42	0.005	0.006	0.22	0.20	0.23
D60	2.408	5.66	0.135	0.269	4.58	3.44	1.42
	0.018	0.37	0.005	0.006	0.19	0.17	0.21
D61	2.156	4.62	0.124	0.269	4.30	3.19	2.06
	0.023	0.46	0.006	0.007	0.24	0.21	0.25
D62	2.276	5.34	0.123	0.280	4.83	3.16	1.56
	0.019	0.38	0.005	0.006	0.20	0.18	0.21
D63	2.261	5.44	0.105	0.236	4.08	2.76	1.85
	0.015	0.26	0.003	0.004	0.14	0.12	0.14
D64	2.170	5.51	0.096	0.230	3.97	3.13	1.68
	0.021	0.42	0.005	0.006	0.22	0.20	0.23
D68	2.512	6.23	0.164	0.338	5.55	3.55	1.57
	0.013	0.24	0.003	0.004	0.12	0.11	0.13
D69	2.379	5.63	0.148	0.304	4.67	2.72	1.67
	0.021	0.41	0.005	0.006	0.22	0.20	0.23
D75	2.117	4.84	0.123	0.282	5.01	3.50	1.86
	0.026	0.50	0.006	0.008	0.26	0.23	0.27
D76 ^b	2.160	4.62	0.075	0.207	3.57	2.52	1.62
	0.042	0.66	0.008	0.010	0.35	0.31	0.36
D78	2.231	4.97	0.120	0.259	4.36	3.09	1.55
	0.025	0.51	0.006	0.008	0.26	0.24	0.28
A3381:										
D19	1.897	...	1.05	1.15	6.45	0.045	0.162	3.27	1.92	...
	0.082	...	0.49	0.34	0.95	0.012	0.014	0.52	0.47	...
D20 ^{b,e}	1.980	...	1.61	1.93	3.47	0.080	0.185	2.86	2.85	...
	0.041	...	0.28	0.19	0.56	0.007	0.008	0.30	0.26	...
D21	2.294	...	1.53	1.86	5.19	0.148	0.303	4.96	3.29	...
	0.017	...	0.16	0.11	0.31	0.004	0.005	0.16	0.15	...
D25	2.306	6.03	1.87	2.29	4.94	0.137	0.288	4.18	3.05	1.52
	0.023	0.74	0.30	0.20	0.61	0.008	0.009	0.32	0.29	0.34
D28	2.146	...	2.29	2.47 ^c	6.94	0.114	0.254	3.90	2.83	...
	0.024	...	0.20	0.18	0.41	0.005	0.006	0.22	0.20	...
D33	2.292	6.05	2.03	2.23	5.13	0.102	0.237	4.16	3.00	1.89
	0.019	0.66	0.22	0.15	0.44	0.005	0.007	0.23	0.21	0.30
D34 ^c	2.376	...	2.73	2.95	1.17	0.107	0.244	4.60	2.89	...
	0.034	...	0.33	0.23	0.72	0.008	0.010	0.36	0.33	...
D37	1.981	...	2.08	2.21	3.77	0.092	0.210	3.58	2.61	...
	0.058	...	0.38	0.26	0.78	0.009	0.011	0.41	0.36	...
D46 ^{a,e}	2.068	3.79	0.091	0.218	3.89	2.47	...
	0.049	0.68	0.008	0.010	0.35	0.32	...
D47 ^{a,e}	1.909	4.15	0.074	0.156	3.14	2.00	...
	0.050	0.48	0.006	0.007	0.26	0.23	...
D48 ^{a,e}	2.180	5.24	0.112	0.249	4.09	2.87	...
	0.020	0.35	0.004	0.005	0.18	0.16	...
D50 ^{b,e}	2.111	...	1.22	1.62	5.53	0.096	0.248	4.17	2.01	...
	0.041	...	0.28	0.19	0.56	0.007	0.008	0.29	0.27	...
D55	2.336	...	1.64	1.95	6.18	0.159	0.322	4.95	3.25	...
	0.018	...	0.19	0.13	0.38	0.005	0.006	0.20	0.18	...
D56	2.342	...	1.66	1.99	5.59	0.151	0.309	5.22	3.33	...
	0.030	...	0.30	0.20	0.59	0.007	0.009	0.30	0.28	...
D64	2.138	...	1.84	1.93	2.94	0.094	0.187	3.58	2.69	...
	0.061	...	0.48	0.33	0.99	0.012	0.014	0.52	0.46	...
D67	2.063	...	2.32	2.47	4.98	0.122	0.251	4.53	2.88	...
	0.058	...	0.43	0.29	0.89	0.011	0.013	0.46	0.42	...
D68	2.194	4.77	2.02	2.61	5.36	0.121	0.283	4.58	3.28	1.44
	0.037	1.16	0.47	0.32	0.95	0.012	0.014	0.50	0.44	0.53
D69 ^{b,e}	2.060	...	-1.01	-0.39 ^c	4.21	0.093	0.196	3.82	2.25	...
	0.074	...	0.49	0.43	0.93	0.011	0.014	0.49	0.44	...
D72 ^b	1.856	...	2.27	2.45 ^c	4.69	0.055	0.175	2.30	2.98	...
	0.108	...	0.53	0.46	1.08	0.013	0.016	0.59	0.50	...
D73	2.125	...	-0.43	0.11	6.34	0.051	0.243	4.70	2.24	...
	0.084	...	0.70	0.48	1.32	0.016	0.020	0.69	0.64	...

TABLE A1—*Continued*

Galaxy	$\log \sigma$	C4668	H β	H β_{G}	Fe5015	Mg ₁	Mg ₂	Mgb	< Fe >	Fe5406
D75	2.339	...	1.85	2.16	4.06	0.144	0.269	4.25	2.85	...
	0.026	...	0.25	0.17	0.51	0.006	0.008	0.27	0.24	...
D76 ^a	2.285	...	2.15	2.63	5.43	...	0.286 ^d	4.53
	0.046	...	0.36	0.24	0.72	...	0.027	0.38
D91 ^a	1.959	7.92	0.064	0.225	5.02	2.85	...
	0.089	1.18	0.015	0.018	0.63	0.57	...
D100	2.310	6.76	1.74	2.13	5.07	0.133	0.284	4.43	2.47	1.51
	0.028	0.83	0.35	0.23	0.70	0.009	0.011	0.36	0.33	0.38
D112	2.347	8.91	2.18	2.40	3.41	0.130	0.288	4.16	2.49	0.93
	0.029	0.82	0.34	0.23	0.71	0.009	0.011	0.37	0.33	0.39
A3574:										
W22	2.330	...	1.14	1.45	4.84	0.151	0.308	4.87	2.48	2.12
	0.017	...	0.21	0.14	0.41	0.005	0.006	0.21	0.19	0.22
W39	2.166	...	1.75	1.96	5.86	0.119	0.259	4.08	2.99	1.84
	0.021	...	0.26	0.18	0.52	0.006	0.008	0.27	0.25	0.28
W47	2.392	...	1.69	1.87	5.86	0.155	0.325	4.55	2.60	1.73
	0.018	...	0.21	0.14	0.41	0.005	0.006	0.22	0.20	0.23
W60 ^e	2.349	...	1.35	1.63	5.10	0.110	0.261	4.48	2.91	1.54
	0.022	...	0.24	0.16	0.48	0.006	0.007	0.25	0.23	0.26
W69 ^e	1.935	4.09	2.40	2.69	4.70	0.064	0.170	2.57	2.20	1.44
	0.026	0.52	0.21	0.14	0.43	0.005	0.006	0.23	0.20	0.23
W74	2.320	...	1.77	1.91	5.32	0.149	0.299	4.96	2.79	1.84
	0.017	...	0.21	0.15	0.43	0.005	0.007	0.22	0.20	0.23
W81	2.271	...	1.38	1.79	5.73	0.127	0.289	4.78	2.56	1.70
	0.019	...	0.23	0.16	0.46	0.006	0.007	0.24	0.22	0.25
S639:										
E264G23	2.342	4.75	...	0.292 ^d	4.62	2.69	2.15
	0.018	0.35	...	0.013	0.18	0.16	0.19
E264G24	2.349	6.26	2.33	2.46	5.96	0.120	0.273	4.37	3.17	1.99
	0.010	0.74	0.30	0.21	0.22	0.003	0.003	0.11	0.10	0.12
E264G26	2.115	5.72	0.111	0.243	4.18	2.86	1.82
	0.025	0.44	0.006	0.007	0.23	0.21	0.24
E264G28	2.191	5.40	0.100	0.242	4.26	3.09	2.17
	0.017	0.36	0.004	0.005	0.19	0.17	0.19
E264G300	2.449	6.82	1.75	2.02	5.64	0.169	0.315	4.69	2.90	1.75
	0.023	0.61	0.25	0.17	0.51	0.006	0.008	0.27	0.24	0.28
E264G301	2.265	4.33	2.56	2.51	5.07	0.111	0.280	4.09	3.14	1.89
	0.015	0.92	0.36	0.25	0.30	0.009	0.011	0.16	0.14	0.16
E264G302	2.276	4.61	0.129	0.262	4.39	2.65	1.99
	0.022	0.42	0.005	0.006	0.22	0.20	0.23
E264G31	2.392	5.67	0.135	0.283	4.77	3.23	2.25
	0.014	0.32	0.004	0.005	0.16	0.15	0.17
J06 ^b	2.041	4.16	0.087	0.201	3.69	2.53	1.17
	0.040	0.61	0.007	0.009	0.32	0.28	0.33
J09 ^e	1.852	5.47	0.118	0.210	4.24	1.82	1.95
	0.105	1.22	0.015	0.018	0.64	0.59	0.67
J10	1.856	4.76	0.074	0.192	3.19	2.90	1.59
	0.061	0.77	0.009	0.011	0.41	0.36	0.42
J13	2.298	3.71	1.75	2.25	5.02	0.119	0.263	4.39	2.96	1.65
	0.013	0.76	0.31	0.21	0.26	0.003	0.004	0.14	0.12	0.14
J14	2.135	5.28	...	0.244 ^d	3.90	2.77	1.64
	0.023	0.44	...	0.019	0.23	0.21	0.24
J15	2.105	4.60	...	0.207 ^d	3.42	2.64	1.86
	0.020	0.36	...	0.018	0.19	0.17	0.20
J16	2.094	6.69	...	0.253 ^d	4.04	2.85	1.72
	0.027	0.53	...	0.022	0.29	0.26	0.30
J18	1.935	5.71	...	0.223 ^d	3.62	1.97	2.31
	0.077	1.26	...	0.057	0.68	0.61	0.68
J20	1.633	7.05	...	0.181 ^d	3.12	1.61	1.49
	0.134	0.94	...	0.051	0.52	0.47	0.53
J23 ^b	2.140	4.43	0.110	0.249	4.42	2.52	2.03
	0.034	0.58	0.007	0.009	0.30	0.27	0.31
J26	2.496	5.72	0.148	0.303	5.30	3.05	2.16
	0.019	0.36	0.005	0.006	0.19	0.17	0.20
J32	2.187	5.75	0.119	0.267	4.33	3.23	1.91
	0.017	0.35	0.004	0.005	0.19	0.17	0.20
J101	1.960	5.91	0.078	0.210	3.83	2.64	2.39
	0.042	0.65	0.008	0.010	0.35	0.31	0.35
J104 ^e	2.018	4.30	0.065	0.137	2.95	1.61	1.25
	0.068	0.67	0.008	0.010	0.36	0.32	0.37
J109	2.154	6.14	0.095	0.252	4.08	3.17	2.10
	0.019	0.39	0.005	0.006	0.21	0.19	0.22
S753:										
W08 ^b	2.055	...	1.56	1.89	4.82	0.086	0.234	3.72	2.80	1.71
	0.020	...	0.25	0.17	0.50	0.006	0.008	0.26	0.24	0.27

TABLE A1—*Continued*

Galaxy	$\log \sigma$	C4668	H β	H β_{G}	Fe5015	Mg ₁	Mg ₂	Mgb	< Fe >	Fe5406
W10	2.100	...	1.87	2.25	4.68	0.090	0.226	3.49	2.73	1.49
	0.017	...	0.19	0.13	0.39	0.005	0.006	0.21	0.18	0.21
W12	2.201	...	1.33	1.77	5.10	0.131	0.282	4.14	2.87	2.08
	0.018	...	0.24	0.17	0.48	0.006	0.007	0.25	0.23	0.26
W17	1.993	...	2.21	2.28	5.13	0.078	0.197	3.04	2.12	1.44
	0.026	...	0.26	0.18	0.53	0.006	0.008	0.29	0.25	0.29
W26	2.154	...	1.74	1.98	4.78	0.097	0.245	3.85	2.87	1.87
	0.018	...	0.23	0.16	0.46	0.006	0.007	0.24	0.22	0.25
W29	2.420	...	0.85	1.46	5.33	0.154	0.305	4.69	3.08	1.80
	0.024	...	0.25	0.17	0.50	0.006	0.008	0.26	0.23	0.27
W37	2.222	...	1.55	1.87	4.80	0.142	0.298	4.28	2.49	1.33
	0.020	...	0.20	0.14	0.40	0.005	0.006	0.21	0.19	0.22
W39 ^a	2.332	7.68	1.17	1.52	4.12	0.132	0.280	4.19	3.14	...
	0.028	0.69	0.30	0.20	0.59	0.007	0.009	0.31	0.27	...
W47	2.067	...	2.33	2.50	5.24	0.096	0.249	3.84	2.59	1.50
	0.031	...	0.34	0.23	0.68	0.008	0.010	0.36	0.32	0.38
W49	2.387	...	1.89	2.06	5.18	0.132	0.302	4.97	2.68	1.73
	0.019	...	0.20	0.14	0.41	0.005	0.006	0.21	0.19	0.22
W51	2.171	...	1.68	2.10	5.44	0.114	0.247	4.12	2.70	1.77
	0.024	...	0.31	0.21	0.62	0.008	0.009	0.32	0.29	0.34
W54	2.248	...	2.09	2.16	5.56	0.117	0.260	4.26	2.58	1.56
	0.018	...	0.20	0.14	0.40	0.005	0.006	0.21	0.19	0.22
W64	2.522	...	1.56	1.79	5.57	0.169	0.335	5.28	3.03	1.96
	0.017	...	0.17	0.12	0.34	0.004	0.005	0.18	0.16	0.19
W73	2.260	...	1.47	1.81	5.38	0.147	0.301	4.37	2.60	1.62
	0.019	...	0.23	0.15	0.45	0.006	0.007	0.24	0.21	0.25
W84	2.318	...	1.50	1.59	5.60	0.136	0.294	4.61	2.97	2.20
	0.024	...	0.28	0.19	0.56	0.007	0.009	0.29	0.26	0.30
W95	2.108	...	1.78	1.91	5.19	0.109	0.259	4.25	2.93	1.65
	0.020	...	0.24	0.16	0.47	0.006	0.007	0.25	0.22	0.26
Doradus:										
A0426-54 ^e	1.653	...	2.25	2.21	2.21	0.011	0.086	1.81	1.14	0.75
	0.102	...	0.33	0.22	0.68	0.008	0.009	0.36	0.32	0.37
N1411 ^e	2.099	...	1.83	2.04	4.39	0.085	0.213	3.65	2.57	1.66
	0.013	...	0.12	0.08	0.25	0.003	0.004	0.13	0.12	0.13
N1527	2.198	...	1.79	1.98	5.36	0.118	0.260	4.07	2.77	1.59
	0.012	...	0.14	0.10	0.29	0.004	0.004	0.15	0.14	0.16
N1533 ^e	2.243	...	1.18	1.37	3.59	0.129	0.282	4.27	2.53	1.70
	0.024	...	0.30	0.21	0.61	0.007	0.009	0.31	0.28	0.33
N1543	2.158	...	1.68	2.04	5.74	0.116	0.277	4.09	2.88	1.75
	0.014	...	0.18	0.12	0.35	0.004	0.005	0.18	0.17	0.19
N1549	2.293	...	1.61	1.99	4.68	0.126	0.263	3.99	2.86	1.67
	0.018	...	0.20	0.14	0.40	0.005	0.006	0.21	0.19	0.22
N1553 ^{b,e}	2.215	...	1.69	1.97	5.25	0.113	0.264	3.88	2.78	1.77
	0.020	...	0.24	0.17	0.48	0.006	0.007	0.25	0.23	0.27
N1574	2.313	...	1.55	1.93	4.36	0.118	0.287	4.41	2.63	1.90
	0.020	...	0.25	0.17	0.51	0.006	0.008	0.26	0.24	0.28
N1596 ^e	2.196	...	1.65	1.89	4.83	0.115	0.271	4.50	2.64	1.78
	0.016	...	0.17	0.12	0.35	0.004	0.005	0.18	0.16	0.19
Grm15:										
A1959-56	2.419	...	1.56	1.83	5.02	0.156	0.332	4.81	3.20	1.76
	0.024	...	0.28	0.19	0.56	0.007	0.009	0.29	0.26	0.31
I4944 ^{b,e}	2.080	4.54	1.10	1.02	4.44	0.046	0.159	2.77	1.86	1.52
	0.041	0.67	0.28	0.19	0.55	0.007	0.008	0.30	0.26	0.30
I4952 ^{b,e}	2.123	...	1.74	2.21	4.30	0.088	0.225	3.38	2.49	1.71
	0.030	...	0.25	0.17	0.51	0.006	0.008	0.27	0.24	0.28
N6848 ^e	2.256	...	1.67	1.97	5.08	0.113	0.240	3.39	3.12	1.81
	0.021	...	0.26	0.17	0.51	0.006	0.008	0.27	0.24	0.28
N6850 ^{b,e}	2.248	...	1.99	2.26	4.44	0.094	0.224	3.49	2.84	1.47
	0.013	...	0.15	0.10	0.31	0.004	0.005	0.17	0.15	0.17
N6854	2.328	6.72	1.31	1.68	4.80	0.137	0.301	4.68	2.45	1.45
	0.019	0.41	0.18	0.12	0.35	0.004	0.005	0.18	0.16	0.19
N6855	2.282	...	2.52	2.35	5.21	0.143	0.320	4.98	2.86	1.84
	0.040	...	0.22	0.15	0.44	0.005	0.007	0.23	0.21	0.24
HydraI:										
E436G44	2.213	7.79	1.85	2.27	5.29	0.123	0.258	4.18	2.78	1.70
	0.024	0.73	0.31	0.21	0.62	0.008	0.009	0.32	0.29	0.34
E436G45	2.279	5.66	1.43	1.63	5.26	0.136	0.268	4.34	2.19	1.36
	0.028	0.76	0.32	0.21	0.62	0.008	0.010	0.33	0.30	0.35
E437G11	2.275	5.18	...	0.285 ^d	4.52	2.99	1.80
	0.015	0.29	...	0.011	0.16	0.15	0.16
E437G13	2.224	4.98	...	0.249 ^d	3.97	2.80	2.13
	0.012	0.22	...	0.009	0.12	0.10	0.12
E437G21	2.248	7.02	2.09	2.30	5.75	0.138	0.283	4.06	3.08	1.62
	0.019	0.62	0.26	0.18	0.52	0.007	0.008	0.27	0.25	0.29

TABLE A1—*Continued*

Galaxy	$\log \sigma$	C4668	H β	H β_G	Fe5015	M $_{G1}$	M $_{G2}$	Mgb	< Fe >	Fe5406
E437G45	2.103	6.20	2.37	2.48	3.98	0.128	0.279	4.68	3.03	1.65
	0.031	1.08	0.44	0.30	0.91	0.011	0.014	0.46	0.42	0.49
E501G03	2.323	5.85	1.77	2.05	5.41	0.129	0.285	4.56	2.87	2.33
	0.018	0.62	0.26	0.18	0.52	0.006	0.008	0.27	0.24	0.28
E501G13	2.352	7.75	2.41	2.48	6.62	0.153	0.306	4.67	2.78	1.60
	0.021	0.68	0.28	0.19	0.57	0.007	0.009	0.30	0.27	0.32
E501G27	1.739	5.64	...	0.132 ^d	2.61	2.89	0.97
	0.072	0.62	...	0.040	0.34	0.29	0.35
E501G35	2.172	5.87	...	0.269 ^d	4.27	3.07	2.01
	0.010	0.18	...	0.007	0.10	0.09	0.10
E501G47	2.135	6.10	...	0.287 ^d	4.55	2.78	1.67
	0.015	0.30	...	0.010	0.16	0.14	0.17
E501G49	2.036	6.31	...	0.237 ^d	3.80	3.07	1.42
	0.022	0.41	...	0.017	0.22	0.20	0.23
I0629	2.058	0.239 ^d	3.83	3.03	1.71
	0.020	0.015	0.20	0.18	0.19
I2597	2.388	8.20	2.07	2.16	5.47	0.164	0.318	4.71	3.00	1.83
	0.013	0.51	0.22	0.15	0.25	0.005	0.007	0.14	0.13	0.14
N3305	2.391	5.88	...	0.336 ^d	5.41	3.16	1.97
	0.010	0.15	...	0.005	0.08	0.07	0.08
N3308	2.288	7.04	1.62	1.99	5.57	0.150	0.303	4.80	2.74	2.10
	0.011	0.81	0.34	0.23	0.21	0.009	0.011	0.12	0.11	0.12
N3309	2.418	7.71	1.91	1.93	5.82	0.160	0.336	5.24	3.17	1.79
	0.009	0.85	0.36	0.25	0.16	0.009	0.011	0.08	0.08	0.09
N3311	2.291	7.52	1.80	1.91	5.38	0.171	0.332	5.35	3.20	1.96
	0.015	0.94	0.40	0.27	0.32	0.010	0.012	0.18	0.16	0.17
N3315	2.211	5.37	...	0.249 ^d	3.97	2.78	1.77
	0.015	0.26	...	0.011	0.14	0.13	0.14
N3316	2.228	6.21	...	0.283 ^d	4.49	3.03	1.92
	0.012	0.22	...	0.008	0.12	0.11	0.12
R213	1.997	6.57	...	0.279 ^d	4.43	3.30	1.88
	0.017	0.32	...	0.012	0.18	0.16	0.18
R219	2.023	5.90	...	0.260 ^d	4.13	2.89	2.09
	0.022	0.40	...	0.015	0.21	0.19	0.22
R224 ^e	2.013	4.59	...	0.257 ^d	4.09	3.20	1.69
	0.033	0.45	...	0.017	0.23	0.21	0.24
R225	1.937	5.74	...	0.246 ^d	3.94	3.03	1.73
	0.031	0.50	...	0.020	0.27	0.24	0.28
R231	1.942	4.79	...	0.225 ^d	3.65	2.73	1.85
	0.031	0.47	...	0.020	0.25	0.22	0.25
R245	2.068	5.86	...	0.231 ^d	3.72	3.06	2.02
	0.020	0.37	...	0.017	0.21	0.18	0.20
R253	1.904	4.91	...	0.221 ^d	3.59	3.16	1.96
	0.034	0.52	...	0.023	0.27	0.24	0.28
R254	1.661	5.68	...	0.222 ^d	3.61	2.53	1.76
	0.098	0.71	...	0.031	0.38	0.34	0.39
R261 ^e	1.816	0.198 ^d	3.31	2.78	1.21
	0.079	0.036	0.40	0.35	0.41
R293	1.643	3.71	...	0.273 ^d	4.33	2.49	1.51
	0.124	1.05	...	0.036	0.54	0.49	0.57
R303	1.967	0.202 ^d	3.36	2.60	1.33
	0.037	0.022	0.25	0.22	0.26
R308	2.086	5.39	...	0.277 ^d	4.39	2.47	1.68
	0.027	0.41	...	0.015	0.22	0.20	0.23
R319	1.865	5.45	...	0.207 ^d	3.42	2.67	1.26
	0.050	0.60	...	0.028	0.32	0.28	0.33
R327	1.966	4.74	...	0.263 ^d	4.17	2.26	2.08
	0.045	0.64	...	0.024	0.33	0.30	0.35
R338	1.750	5.76	...	0.233 ^d	3.75	2.39	1.09
	0.074	0.66	...	0.028	0.35	0.32	0.37
RMH26	2.024	0.240 ^d	3.85	2.51	1.61
	0.019	0.015	0.19	0.17	0.18
RMH28	2.148	6.54	2.16	2.30	4.37	0.137	0.273	4.39	3.18	1.79
	0.020	0.89	0.37	0.25	0.46	0.009	0.011	0.24	0.21	0.25
RMH29	2.184	5.05	...	0.272 ^d	4.32	2.63	1.31
	0.018	0.32	...	0.013	0.18	0.16	0.18
RMH30 ^a	2.286	...	1.47	1.76 ^c	4.46	0.115	0.272	4.59	2.30	...
	0.021	...	0.23	0.20	0.42	0.006	0.007	0.24	0.22	...
RMH35	2.090	4.87	...	0.283 ^d	4.49	2.92	1.77
	0.015	0.28	...	0.010	0.15	0.13	0.15
RMH50	1.963	4.66	...	0.244 ^d	3.90	2.60	1.64
	0.022	0.32	...	0.014	0.18	0.16	0.17
RMH72	2.076	5.10	1.83	1.99	4.70	0.115	0.250	4.24	2.68	1.67
	0.014	0.77	0.32	0.22	0.27	0.008	0.010	0.15	0.13	0.15
RMH79	2.268	0.271 ^d	4.30	2.62	1.52
	0.015	0.009	0.12	0.11	0.13

TABLE A1—Continued

Galaxy	$\log \sigma$	C4668	H β	H β_G	Fe5015	Mg ₁	Mg ₂	Mgb	< Fe >	Fe5406
Other:										
E462G15	2.459	7.32	1.62	1.90	5.24	0.132	0.292	4.48	3.00	1.93
	0.026	0.68	0.29	0.19	0.57	0.007	0.009	0.30	0.27	0.31
E553G02	2.406	7.71	1.18	1.10	6.50	0.136	0.279	4.23	2.47	1.65
	0.060	1.52	0.65	0.45	1.27	0.016	0.020	0.68	0.61	0.71
H86A	2.398	8.59	1.20	1.53	5.68	0.172	0.336	5.11	3.12	1.79
	0.024	0.60	0.26	0.18	0.51	0.006	0.008	0.26	0.24	0.28
H86B	2.313	6.72	1.70	1.72	5.54	0.137	0.288	4.13	2.34	1.49
	0.026	0.62	0.26	0.18	0.51	0.006	0.008	0.27	0.25	0.29
H86C	2.239	3.74	0.82	1.20	4.49	0.129	0.307	5.34	3.26	1.50
	0.036	1.17	0.49	0.33	0.95	0.012	0.015	0.48	0.44	0.52
H86D	2.274	7.77	1.94	2.18	5.14	0.134	0.286	4.33	2.85	1.71
	0.025	0.53	0.22	0.15	0.45	0.006	0.007	0.23	0.21	0.25
H90B	2.410	...	1.70	2.07	5.18	0.150	0.318	4.72	3.08	2.83
	0.023	...	0.28	0.19	0.56	0.007	0.009	0.29	0.26	0.30
H90C	2.266	...	1.67	2.00	4.95	0.137	0.285	4.53	2.69	1.60
	0.019	...	0.22	0.15	0.45	0.006	0.007	0.23	0.21	0.25
H90D ^e	2.132	...	0.56	0.87	3.64	0.065	0.185	3.22	3.01	1.35
	0.032	...	0.31	0.21	0.61	0.007	0.009	0.32	0.28	0.33
H98A	2.396	8.01	2.10	2.37	6.01	0.134	0.289	4.66	2.77	2.06
	0.020	0.56	0.23	0.16	0.47	0.006	0.007	0.25	0.22	0.26
H98B	2.390	8.84	1.83	1.93	4.13	0.132	0.305	5.05	2.76	1.74
	0.023	0.59	0.25	0.17	0.51	0.006	0.008	0.26	0.24	0.28
I2006 ^e	2.070	...	1.89	2.03	4.50	0.119	0.262	4.17	2.67	1.75
	0.015	...	0.18	0.12	0.35	0.004	0.005	0.18	0.17	0.19
N0720	2.361	...	1.23	1.59	5.57	0.161	0.326	4.74	2.83	1.99
	0.015	...	0.17	0.11	0.33	0.004	0.005	0.17	0.16	0.18
N1339	2.205	...	1.69	1.95	5.67	0.137	0.296	4.37	2.64	1.72
	0.019	...	0.22	0.15	0.44	0.006	0.007	0.23	0.21	0.24
N1395	2.375	...	2.00	2.23	4.54	0.152	0.316	4.38	2.67	1.95
	0.018	...	0.18	0.12	0.36	0.005	0.006	0.19	0.17	0.20
N1399	2.535	...	1.12	1.61	5.72	0.176	0.331	5.48	3.11	2.37
	0.022	...	0.26	0.18	0.52	0.007	0.008	0.27	0.24	0.28
N1403	2.199	...	1.83	2.12	4.43	0.109	0.250	4.10	2.82	1.10
	0.024	...	0.30	0.20	0.60	0.007	0.009	0.31	0.28	0.33
N1426	2.170	...	1.65	1.96	4.30	0.105	0.251	3.75	2.55	1.76
	0.020	...	0.24	0.16	0.48	0.006	0.007	0.25	0.23	0.26
N1439	2.120	8.71	2.27	2.51	5.37	0.142	0.282	4.20	2.60	1.73
	0.019	0.86	0.25	0.17	0.49	0.006	0.008	0.26	0.23	0.27
N1600	2.472	7.49	0.88	1.44	5.25	0.176	0.334	4.93	3.03	1.90
	0.030	0.81	0.35	0.24	0.69	0.009	0.011	0.36	0.32	0.38
N1726	2.387	7.27	1.16	1.67	4.72	0.148	0.291	4.61	2.70	2.02
	0.016	0.51	0.22	0.15	0.43	0.005	0.007	0.22	0.20	0.23
N1794 ^e	2.270	4.68	0.04	0.26	4.22	0.106	0.218	3.81	2.76	1.52
	0.030	0.69	0.29	0.20	0.57	0.007	0.008	0.30	0.27	0.31
N2293	2.397	...	1.47	1.77	4.72	0.142	0.308	4.89	3.25	2.01
	0.014	...	0.18	0.13	0.37	0.005	0.006	0.19	0.17	0.20
N2513	2.469	8.79	2.26	2.38	6.31	0.167	0.314	5.03	3.33	2.02
	0.026	0.76	0.32	0.22	0.64	0.008	0.010	0.33	0.30	0.35
N2865	2.216	...	3.17	3.23	5.66	0.086	0.199	3.05	2.68	1.35
	0.018	...	0.19	0.13	0.38	0.005	0.006	0.21	0.18	0.21
N2974 ^e	2.408	8.59	0.89	1.19	4.41	0.154	0.291	4.64	2.92	1.88
	0.013	0.35	0.15	0.10	0.30	0.004	0.005	0.16	0.14	0.16
N2986	2.381	10.00	1.65	1.91	5.35	0.158	0.325	5.04	2.81	1.64
	0.015	0.68	0.18	0.12	0.35	0.004	0.005	0.18	0.17	0.19
N3377	2.132	...	1.98	2.29	4.60	0.112	0.242	3.64	2.50	1.63
	0.013	...	0.14	0.10	0.29	0.004	0.004	0.15	0.14	0.16
N3379	2.300	8.22	1.59	1.86	5.05	0.151	0.304	4.79	2.40	1.90
	0.015	0.39	0.17	0.11	0.33	0.004	0.005	0.17	0.16	0.18
N5898 ^e	2.362	...	1.70	1.89	5.63	0.137	0.300	4.47	2.80	2.09
	0.012	...	0.14	0.09	0.27	0.003	0.004	0.14	0.13	0.15
N5903	2.292	...	1.51	1.71	5.02	0.126	0.281	4.68	2.93	2.03
	0.016	...	0.21	0.14	0.42	0.005	0.006	0.22	0.20	0.23
N6849	2.301	8.22	1.39	1.81	4.90	0.124	0.272	4.29	2.43	1.92
	0.026	0.72	0.31	0.21	0.61	0.008	0.009	0.32	0.29	0.33
N7619	2.472	...	1.67	1.96	5.23	0.163	0.329	4.83	2.89	1.85
	0.016	...	0.16	0.11	0.32	0.004	0.005	0.17	0.15	0.18
N7626	2.423	...	1.64	1.80	5.11	0.158	0.315	5.13	3.17	2.02
	0.017	...	0.20	0.14	0.40	0.005	0.006	0.20	0.19	0.22

NOTE.— ^a Not member of the cluster, cf. Paper I. ^b Classified as spiral, cf. Jørgensen et al. (1995a).
^c Eq. 1 used to derive H β_G from H β . ^d Eq. A3 used to derive Mg₂ from Mgb. ^e Significant emission lines.
< Fe > = (Fe5270+Fe5335)/2. Internal uncertainties are given in the second line for each galaxy. All
parameters, except H β in emission, have been aperture corrected to a circular aperture with diameter
 $2r_{\text{a,orm}} = 1.19h^{-1}\text{kpc}$, equivalent to $3''/4$ at the distance of the Coma cluster. The line indices are consistent
with the Lick/IDS system and corrected to zero velocity dispersion.

unconvolved spectrum and the convolved spectrum as function of the velocity dispersion was fitted with a low-order polynomial, as done for Mg_2 in Paper I. For the other indices the quotient between the index from the unconvolved spectrum and the convolved spectrum was used. At 200 km s^{-1} the corrections are 0.002 for Mg_2 , 2% for $\text{H}\beta_{\text{G}}$ and 15% for $\langle \text{Fe} \rangle$. The signs and sizes of the corrections agree with the corrections used by Davies et al. (1993) for the indices in common.

A4 Internal comparison

Figure A1 and Table A3 summarize the internal comparisons of the line indices. Small offsets were applied to the OPTOPUS data for some indices as follows. $\text{Mgb}_{\text{B\&C}} = \text{Mgb}_{\text{OPTOPUS}} + 0.30$, $\text{Fe5015}_{\text{B\&C}} = \text{Fe5015}_{\text{OPTOPUS}} + 0.31$, $\text{Fe5270}_{\text{B\&C}} = \text{Fe5270}_{\text{OPTOPUS}} + 0.28$, $\text{Fe5335}_{\text{B\&C}} = \text{Fe5335}_{\text{OPTOPUS}} + 0.13$, and $\text{Fe5406}_{\text{B\&C}} = \text{Fe5406}_{\text{OPTOPUS}} + 0.12$. These offsets may be caused by poorer flux calibration of the OPTOPUS data.

The rms scatter of the comparisons is in general fully explained by the estimated internal uncertainties, cf. Table 2. It is clear from the comparisons that the new index $\text{H}\beta_{\text{G}}$ has lower uncertainty than the Lick/IDS index for $\text{H}\beta$.

A5 Transformation to Lick/IDS system

The consistency with and transformation to the Lick/IDS system were established by comparison with data from the Lick/IDS project (Faber 1994) and from Gonz  les (1993).

Values from Faber (1994) were aperture corrected with our adopted aperture correction under the assumption that they were all taken with or corrected to the Lick aperture size $1''.5 \times 4''.0$ (equivalent to a circular aperture with diameter $2''.95$, cf. Paper I). Values from Gonz  les (1993) were aperture corrected. The aperture size used by Gonz  les is $2''.1 \times 5''.0$, equivalent to a circular aperture with diameter $3''.75$. The comparisons are done for line indices uncorrected for the velocity dispersion.

The comparisons for some of the indices are shown in Figure A2. Table A4 summarizes all the comparisons. We have 24 galaxies in common with Faber and only 6 galaxies in common with Gonz  les. It is however clear that the scatter for the comparisons with data from Gonz  les is significantly lower than for the comparisons with data from Faber. As also noted by Worthey et al. (1992) the data from Gonz  les are of significantly better quality than the Lick/IDS data. The data from Gonz  les are also of significantly better quality than the data presented in this paper, due to the very high signal-to-noise spectra obtained by Gonz  les. The scatter in the comparisons with Gonz  les can be explained entirely by the internal uncertainty of our data. The galaxy NGC547 is in both comparisons. Our data agree with data from Gonz  les, while the data from Faber show large deviations in some of the indices, see Figure A2.

The only significant offsets between our data and the Lick/IDS system are the offset in Mg_2 , consistent with the offset -0.011 adopted in Paper I, and the offset in Mg_1 . In order to calibrate Mg_1 to the Lick/IDS system we add 0.007 to our values. The data given in Table A1 are offset to the Lick/IDS system.

TABLE A2
SPECTROSCOPIC PARAMETERS, MEAN VALUES

Galaxy	Fe4531	Fe5709	Fe5782	NaD
A539:				
D16	2.59	1.10	0.44	...
	0.51	0.30	0.30	...
A3381:				
D25	2.17	0.69	0.76	...
	0.46	0.27	0.26	...
D33	2.68	1.03	1.17	...
	0.40	0.24	0.23	...
D68	2.30	0.04	1.09	...
	0.71	0.43	0.40	...
D100	3.10	0.34	0.18	...
	0.51	0.31	0.30	...
D112	3.09	0.64	0.58	...
	0.51	0.31	0.30	...
S639:				
E264G24	2.94	0.72	0.54	3.88
	0.46	0.27	0.27	0.31
E264G300	4.00	0.53	-0.06	5.71
	0.37	0.23	0.22	0.25
E264G301	2.31	0.62	1.75	3.77
	0.56	0.33	0.31	0.38
J13	3.07	0.51	0.56	4.52
	0.45	0.27	0.27	0.31
HydraI:				
E436G44	3.46	0.76	0.52	3.13
	0.45	0.27	0.27	0.32
E436G45	2.71	0.54	0.55	3.51
	0.46	0.28	0.27	0.32
E437G21	2.58	0.71	0.69	4.36
	0.39	0.23	0.22	0.26
E437G45	3.41	0.73	0.34	3.56
	0.65	0.39	0.39	0.45
E501G03	2.85	0.54	0.06	3.96
	0.38	0.23	0.23	0.26
E501G13	3.89	0.98	0.73	3.99
	0.42	0.25	0.25	0.29
I2597	2.52	0.73	0.76	5.21
	0.32	0.19	0.19	0.21
N3308	3.11	0.92	0.59	4.73
	0.50	0.30	0.29	0.34
N3309	4.31	0.89	-0.06	4.89
	0.52	0.32	0.32	0.36
N3311	2.94	0.79	0.89	5.22
	0.58	0.35	0.34	0.39
RMH28	2.18	0.72	0.44	2.79
	0.56	0.33	0.32	0.39
RMH72	3.96	1.12	0.45	2.87
	0.46	0.28	0.27	0.33
Other:				
E553G02	1.17	0.52	0.32	4.65
	0.98	0.57	0.56	0.64
N1439	...	0.86	0.66	3.59
	...	0.33	0.32	0.37
N1600	1.78	0.67	0.99	5.23
	0.51	0.30	0.29	0.34
N1726	2.97	1.04	0.34	4.20
	0.31	0.19	0.18	0.21
N1794	2.04	0.99	-0.04	4.42
	0.42	0.25	0.25	0.28
N2513	1.66	0.95	0.44	5.05
	0.49	0.28	0.28	0.32
N2974	...	0.84	0.50	4.65
	...	0.13	0.13	0.15
N2986	...	0.80	0.72	5.41
	...	0.26	0.25	0.29
N3379	...	0.82	0.69	4.33
	...	0.15	0.14	0.16

NOTE.— Internal uncertainties are given in the second line for each galaxy. All line indices have been aperture corrected to a circular aperture with diameter $2r_{\text{norm}} = 1.19h^{-1}\text{kpc}$, equivalent to $3''.4$ at the distance of the Coma cluster. The line indices are consistent with the Lick/IDS system and corrected to zero velocity dispersion.

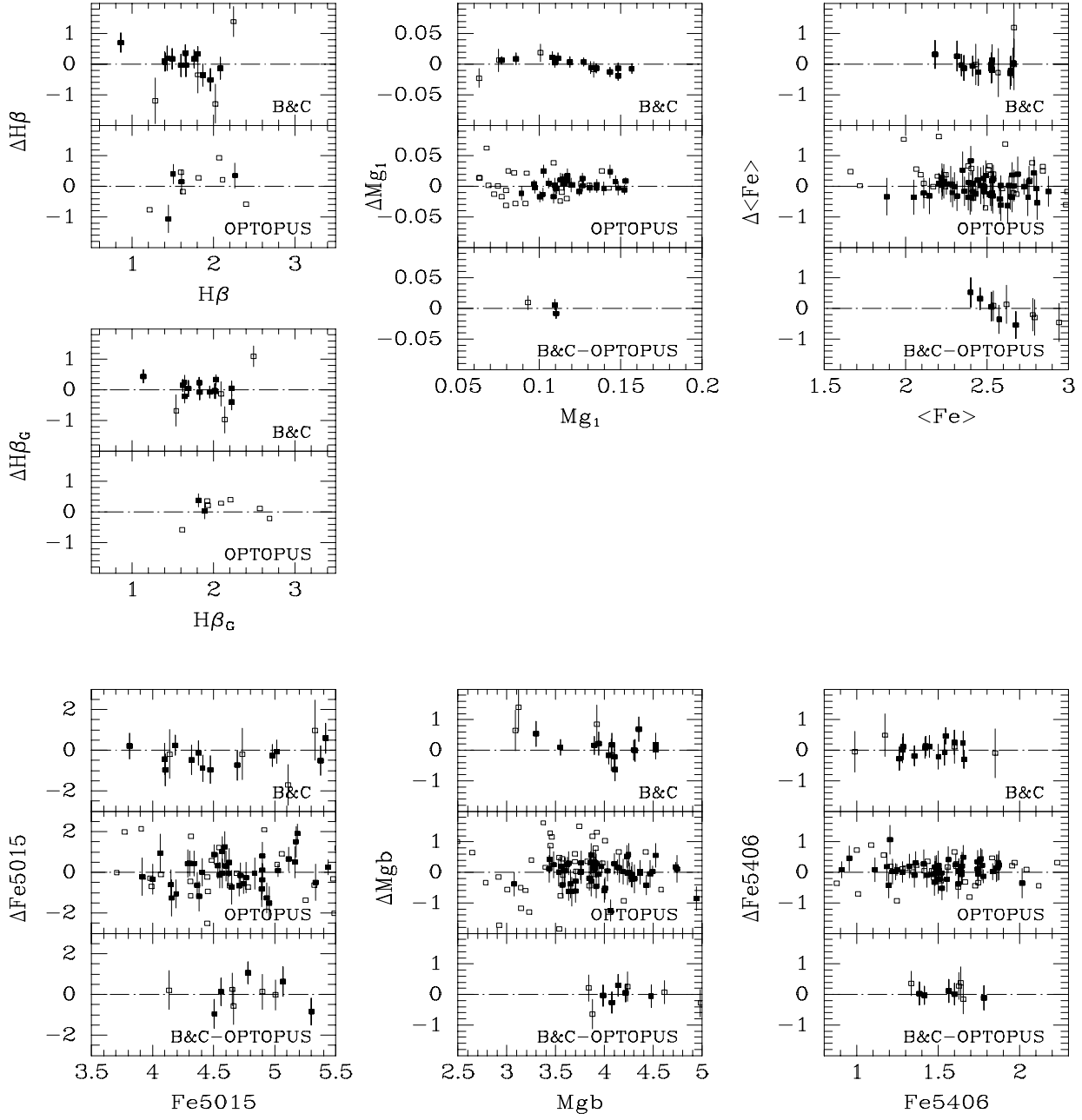


Figure A1. Internal comparison. Solid points – data from spectra with $S/N \geq 20$ per \AA . Open points – data from spectra with $S/N < 20$ per \AA .

Table A3. Internal comparison

Index	B&C		B&C ^a		OPTOPUS		OPTOPUS ^a		B&C-OPTOPUS	
	N _{gal}	rms	N _{gal}	rms	N _{gal}	rms	N _{gal}	rms	N _{gal}	rms
C4668	5	1.48	3	0.50						
H β	17	0.63	13	0.31	11	0.60	4	0.69		
H β _G	17	0.45	13	0.23	9	0.33	2	0.24		
Mg ₁	17	0.011	13	0.009	56	0.017	32	0.010	10	0.29
Mg ₂	17	0.019	13	0.008	56	0.021	32	0.014	3	0.009
Mgb	17	0.48	13	0.33	98	0.62	56	0.37	3	0.007
<Fe>	17	0.35	13	0.19	97	0.43	56	0.30	10	0.35
Fe5406	17	0.24	13	0.23	84	0.35	51	0.27	9	0.20

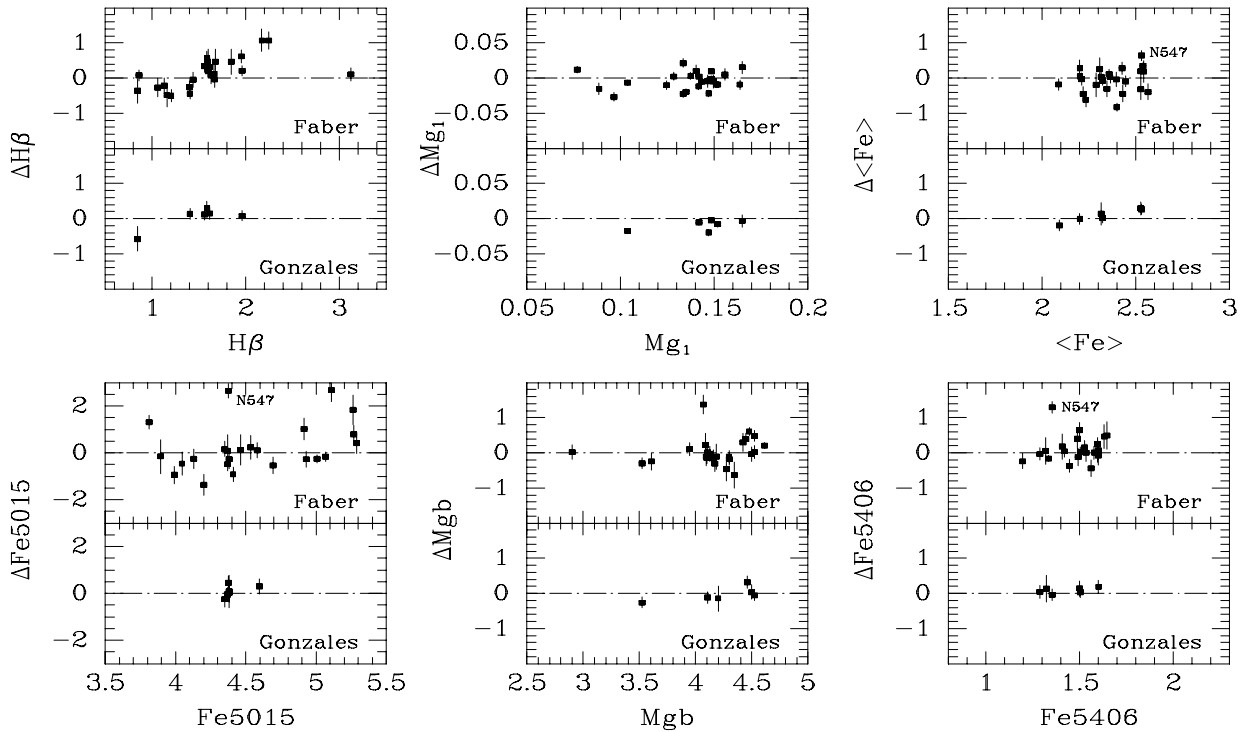
Note – ^a observations with S/N<20 per Å excluded.

Table A4. External comparison

Index	Faber (1994)			Faber (1994) ^a			González (1993)		
	N _{gal}	< Δ >	rms	N _{gal}	< Δ >	rms	N _{gal}	< Δ >	rms
Fe4531	5	-0.57	0.94	4	-0.34	0.91			
C4668	15	0.49	1.90	12	0.07	1.44			
H β	24	0.15	0.44	21	0.09	0.34	6	0.03	0.31
Fe5015	24	0.22	1.04	21	-0.09	0.64	6	0.09	0.25
Mg ₁	24	-0.004	0.013	21	-0.006	0.011	6	-0.009	0.007
Mg ₂	24	-0.008	0.017	21	-0.009	0.012	6	-0.018	0.010
Mgb	24	0.04	0.40	21	-0.02	0.27	6	-0.04	0.20
<Fe>	24	-0.07	0.34	21	-0.09	0.31	6	0.09	0.18
Fe5406	22	0.12	0.37	19	0.06	0.29	6	0.08	0.08
Fe5709	7	0.08	0.18	5	0.13	0.17			
Fe5782	7	-0.22	0.35	5	-0.12	0.28			
NaD	9	-0.40	0.68	5	-0.12	0.22			

Note – Differences < Δ > are calculated as “our”-“literature”.

^a observations with S/N<20 per Å excluded.

**Figure A2.** External comparison. All differences are calculated as “our”-“literature” and plotted versus our determinations.

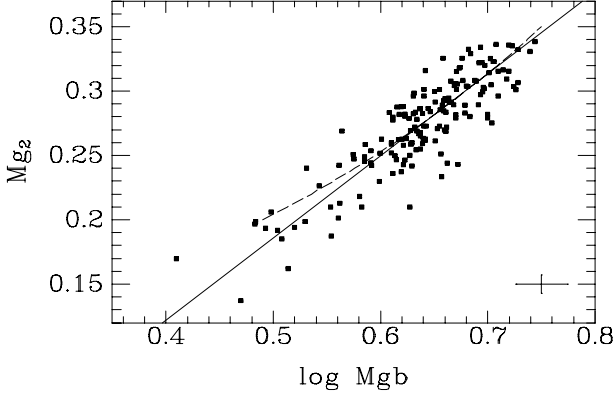


Figure A3. The relation between the Mg_2 index and the Mgb index. Solid line – the relation given in Eq. A3. Dashed line – the relation for E galaxies shown by Burstein et al. (1984).

A6 Correlations between the magnesium indices

The indices Mgb and Mg_2 are strongly correlated. For the 161 E and S0 galaxies with both indices available we find

$$Mg_2 = 0.638 \log Mgb - 0.133 \pm 0.044 \quad (A3)$$

with an rms scatter of 0.019, see Figure A3. For Mg_2 in the interval 0.2–0.35 the relation is in agreement with the relation for E galaxies shown by Burstein et al. (1984). This relation is overplotted on Figure A3. Two galaxies with uncertainty on $\log Mgb$ larger than 0.08 were excluded from the fit. The relation has no significant intrinsic scatter. The relation was therefore used to derive Mg_2 from the measured Mgb for those 37 galaxies where Mg_2 could not be measured because parts of the continuum bands for that index were outside the observed wavelength range.

There is, as expected, a strong correlation between the indices Mg_1 and Mg_2 . We find the following relation for E and S0 galaxies

$$Mg_2 = 1.515 Mg_1 + 0.082 \pm 0.050 \quad (A4)$$

with an rms scatter of 0.015. The derived relation is very similar to the relation for E galaxies shown by Burstein et al. (1984). The relation has no significant intrinsic scatter. Mg_1 is not used in the present analysis, since this index from an observational point of view does not contain additional information.